

Strictly self-similar fractals composed of star-polygons that are attractors of Iterated Function Systems.

Vassil Tzanov

February 6, 2015

Abstract

In this paper are investigated strictly self-similar fractals that are composed of an infinite number of regular star-polygons, also known as Sierpinski n -gons, n -flakes or polyflakes. Construction scheme for Sierpinsky n -gon and n -flake is presented where the dimensions of the Sierpinsky ∞ -gon and the ∞ -flake are computed to be 1 and 2, respectively. These fractals are put in a general context and Iterated Function Systems are applied for the visualisation of the geometric iterations of the initial polygons, as well as the visualisation of sets of points that lie on the attractors of the IFS generated by random walks. Moreover, it is shown that well known fractals represent isolated cases of the presented generalisation. The IFS programming code is given, hence it can be used for further investigations.

1 Introduction - the Cantor set and regular star-polygonal attractors

A classic example of a strictly self-similar fractal that can be constructed by Iterated Function System is the Cantor Set [1]. Let us have the interval $E = [-1, 1]$ and the contracting maps $S_1, S_2 : \mathbb{R} \rightarrow \mathbb{R}$, $S_1(x) = x/3 - 2/3$, $S_2(x) = x/3 + 2/3$, where $x \in E$. Also $S^k : S(S^{k-1}(E)) = S^k(E)$, $S^0(E) = E$, where $S(E) = S_1(E) \cup S_2(E)$. Thus if we iterate the map S infinitely many times this will result in the well known Cantor Set; see figure 1. This iteration procedure can be generalised by the following theorem [2]:

Theorem 1. *If we have $S_1, \dots, S_N : |S_i(x) - S_i(y)| \leq c_i|x - y|$, $c_i < 1$, then \exists unique non-empty set $F : F = \cup_{i=1}^N S_i(F)$, hence invariant for the map S and $F = \cap_{k=1}^{\infty} S^k(E)$*

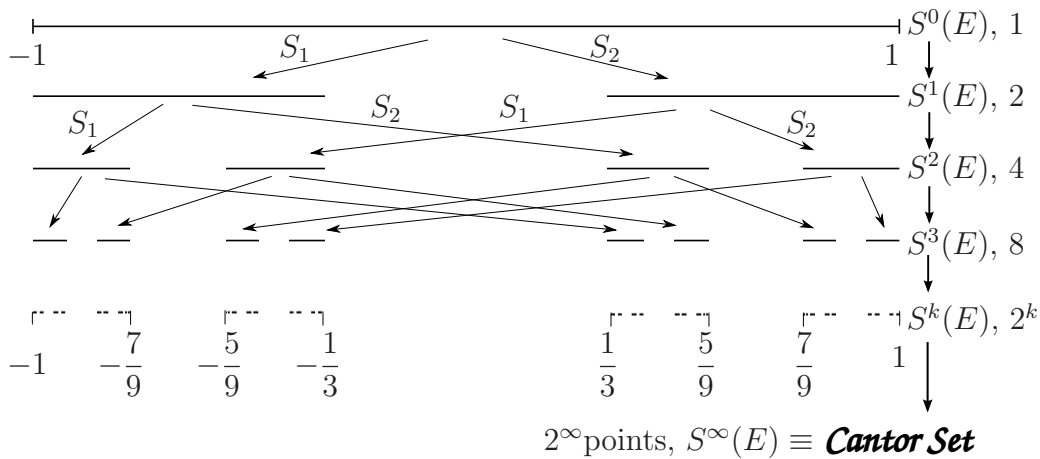


Figure 1: Sketch of the repeated actions of the maps S_1 and S_2 on the interval E that result in the Cantor Set, where the left and right arrows represent S_1 and S_2 , respectively. On the right hand side of the intervals, the corresponding iterations of the map S and the number of the intervals of the particular iteration are shown.

Using a polygon as an initial set for fractal generation is a well known technique since the most famous strictly self-similar fractal examples, the Cantor set and the Sierpinski triangle, consist of infinitely many line-segments and triangles, respectively. In the present paper the number of the vertices of the polygon will be increased to an arbitrary number $n \in \mathbb{N}, n \geq 2$. Thus, the fractal can consist of infinitely many pentagons, hexagons, etc. Furthermore, the building regular polygons will be all $\{n/m\}$ star-polygons [3] where $n \geq 2$ and $m \leq n/2$, $n \in \mathbb{N}$, and $m \in \mathbb{N}$. For our purpose we will take the unit circle and it will be divided in n equal segments. For example, in the case of pentagram, we have $m = 2$ which gives us $\{5/2\}$ -polygon. Once we choose an $\{n/m\}$ -polygon it can be scaled by a factor of $P \in (0, 1)$ with respect to all of the vertices of the polygon. This will produce n new polygons similar to the initial one but scaled down by factor of P . Now, if we repeat the procedure for each one of these new polygons, another n^2 polygons will be created that will be P^2 times smaller than the initial $\{n/m\}$ -polygon inscribed in the unit circle. If the P is chosen carefully, after infinitely

many contractions, the result will be a strictly self-similar fractal composed by non-intersecting polygons. Thus, at the i -th contraction the defined n contracting maps are applied n^i times, and by theorem 1 when $i \rightarrow \infty$ we will define infinitely many points of attraction. These points of attraction specify the attractor of the iteration procedure. This polygonal attractor is a fractal produced by the infinite contractions (n^i , where $i \rightarrow \infty$) of the initial polygon and it is self similar, i.e. it is composed of infinitely many polygons similar to the initial one.

The present study is focused on non-self-intersecting fractals where the scaled copies of the initial polygons osculate with each other. This restricts the possibilities for P when Sierpinsky n -gon [4] for arbitrary n is constructed and a formula about P is derived. This important ratio is reported in two other places [4] and [5] where in the latter the proof is omitted. Moreover, in both manuscripts the authors did not prove that the Hausdorff dimension of the non-self-intersecting ∞ -gon is 1. In the present paper, an original derivation of the equation for the scaling ratio P is presented. It is done in a very detailed way by using simple geometric laws which makes the result affordable even for high-school students. Also, the Hausdorff dimension of the ∞ -gon is shown to be 1. Furthermore, universal constructions for n -flakes are proposed for the cases when n is even or odd, and the Hausdorff dimension of the ∞ -flake is proved to be 2. To this end, formulas for the scaling ratio and the rotation of the central polygon of the n -flake are derived, which to the knowledge of the author have not been reported previously. Finally, it is shown that different initial polygons may result in an identical attractor when an IFS iteration scheme is applied and it is shown which are the main parameters that define the shape of the Sierpinski n -gon and the polyflake attractors.

The paper is constructed as follows: in section 2 the parameters P and m are introduced and an important equation for the ratio $P = P(n, m)$ is derived. In section 3 a condition for m is obtained that ensures no self-intersection of the studied class of fractals. Then, two techniques for imaging IFS attractors are introduced and several Sierpinsky n -gons are computed together with their dimensions. In section 4 the possibility for additional scaling map that scales down towards the centre of the polygon is taken into account. Different constructions for the cases when n is odd or even are proposed so the resulted n -flake to be non-self-intersecting for arbitrary n . Also, a few interesting examples are given and the Hausdorff dimension of the ∞ -flake is computed. In section 5 some well known fractals are shown to be a special case of the fractal generation scheme shown here. It is also explained why identical attractors may originate from different star-polygons and how we can exploit this feature.

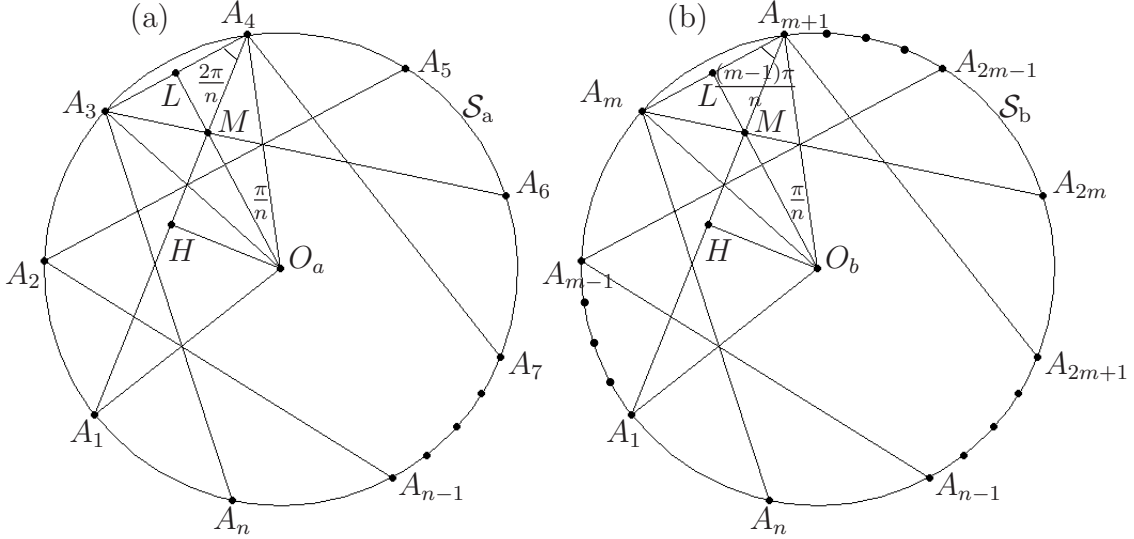


Figure 2: Sketches of $\{n/3\}$ and $\{n/m\}$ star-polygons circumscribed in \mathcal{S}_a and \mathcal{S}_b respectively.

2 The parameters P and m

An important result of the present paper will be explained in this section. Here the scaling parameter P will be deduced from n and m . Therefore, $P = P(n, m)$ is a specific scaling factor for the chosen initial $\{n/m\}$ -polygon, where P does not depend on the diameter of the circumscribed circle.

In figure 2 a sketch of a $\{n/3\}$ star-polygon is shown where $m = 3$. Here, the vertices A_i for $i = 1, \dots, n$ are the vertices of the $\{n/3\}$ star-polygon and O_a is the centre of the circumscribed circle \mathcal{S}_a , M is the intersection point of the secants A_1A_4 and A_3A_6 , H is the orthogonal projection of O_a on A_1A_4 and L is the orthogonal projection of O_a on A_3A_4 . Our purpose will be to find the ratio $P = \frac{MA_4}{A_1A_4}$ because MA_4 will be a line segment of the star-polygon resulted after the scaling of the initial polygon with respect to the point A_4 by factor of P .

The initial polygon is circumscribed by \mathcal{S}_a and O_a is its centre thus $\angle A_3O_aA_4 = 2\pi/n \Rightarrow \angle LO_aA_4 = \pi/n$ because $A_3O_a = A_4O_a$. Also, $\angle A_1O_aA_3 = 4\pi/n \Rightarrow \angle A_1A_4A_3 = 2\pi/n$ and $\angle A_1O_aH = 3\pi/n$, since \mathcal{S}_a with centre at O_a circumscribes A_1 , A_3 and A_4 . Now we can deduce A_1A_4 and A_4M by the radius r of \mathcal{S}_a ; $r = O_aA_i$ for $i = 1, \dots, n$:

$A_1A_4 = 2r \sin(3\pi/n)$. In order to deduce A_4M we will first find A_4L . Thus, $A_4L = r \sin(\pi/n) \Rightarrow A_4M = \frac{A_4L}{\cos(2\pi/n)} = \frac{r \sin(\pi/n)}{\cos(2\pi/n)}$. Now we can substitute the values for A_1A_4 and MA_4 in order to find $P = \frac{MA_4}{A_1A_4} = \frac{\sin(\pi/n)}{2 \cos(2\pi/n) \sin(3\pi/n)}$.

We have just found $P(n, 3)$, now, let us do the same computations for any $1 \leq m \leq n/2$. In figure 2(b) we can find the sketch of a $\{n/m\}$ star-polygon where the vertices A_i for $i = 1, \dots, n$ are the vertices of the star-polygon and O_b is the centre of the circumscribed circle \mathcal{S}_b with radius r , M is the intersection point of the secants A_1A_{m+1} and A_mA_{2m} , H is the orthogonal projection of O_b on A_1A_{m+1} and L is the orthogonal projection of O_b on A_mA_{m+1} . Our purpose will be to find the ratio $P = \frac{MA_{m+1}}{A_1A_{m+1}}$. Thus, $\angle LO_bA_{m+1} = \pi/n$ because $A_mO_b = A_{m+1}O_b$, $\angle A_1O_bA_m = (2m-2)\pi/n \Rightarrow \angle A_1A_{m+1}A_m = (m-1)\pi/n$ and $\angle A_1O_bH = m\pi/n$, since \mathcal{S}_b with centre at O_b circumscribes A_1 , A_m and A_{m+1} . Now we can deduce A_1A_{m+1} and $A_{m+1}M$ by the radius r of \mathcal{S}_b : $A_1A_{m+1} = 2r \sin(m\pi/n)$. In order to deduce $A_{m+1}M$ we will first find $A_{m+1}L$.

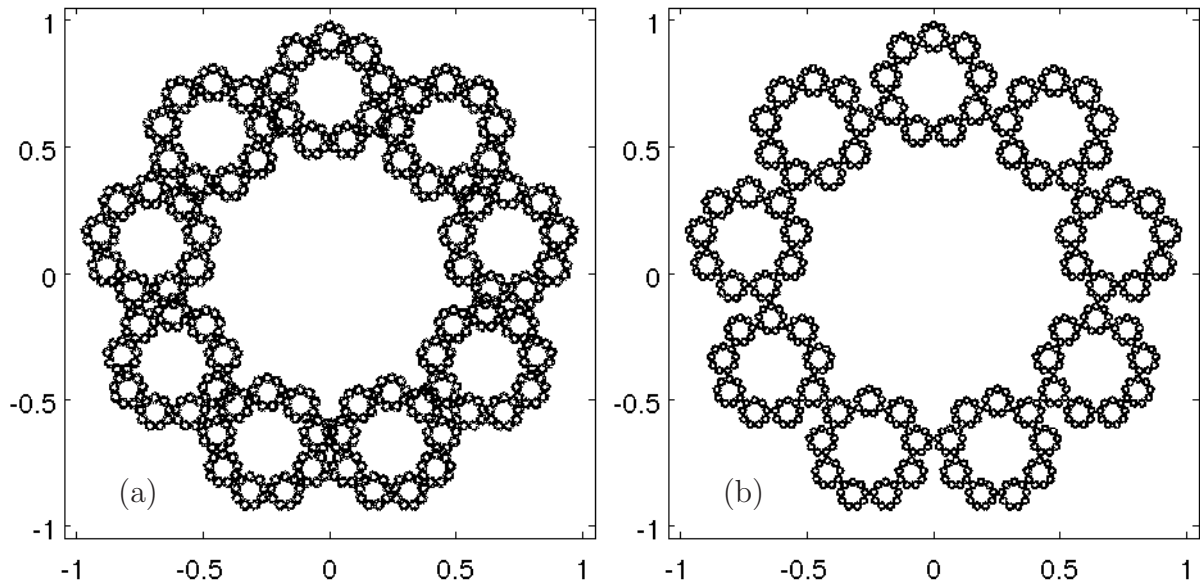


Figure 3: IFS generated fractal sets made of points that lie on $\{9/2\}$ and $\{9/3\}$ star-polygons in subpanels (a) and (b), respectively.

Thus, $A_{m+1}L = r \sin(\pi/n) \Rightarrow A_{m+1}M = \frac{A_{m+1}L}{\cos((m-1)\pi/n)} = \frac{r \sin(\pi/n)}{\cos((m-1)\pi/n)}$ Now we can substitute the values for A_1A_{m+1} and MA_{m+1} in order to find:

$$P = \frac{MA_{m+1}}{A_1A_{m+1}} = \frac{\sin(\pi/n)}{2 \cos((m-1)\pi/n) \sin(m\pi/n)} \quad (1)$$

3 Generation of fractals by using IFS

The values for P obtained in the previous section will be used here for the computation of self-similar fractals that are IFS attractors. These attractors will be derived by the random walk/orbit method or so called chaos game [6, 7]. First, we define a matrix that specifies how many points along the unit circle will be taken into account (n), and what is the contraction $P(n, m)$ towards those points. For example, the matrices for the fractals in figures 3(a) and 3(b) are bellow; see Table 3.

This matrix is then plugged into the random generator, where the number of points that we want to map over the IFS attractor are specified; see the Appendix section 5 for the MATLAB code.

3.1 Condition for non-self-intersection

In figure 3 two examples of star-polygon fractals with initial $\{9/2\}$ - and $\{9/3\}$ -polygons clarify why the parameter m in the ratio $\frac{MA_{m+1}}{A_1A_{m+1}}$ is important when non-self-intersecting fractals are desired. We would like the self-intersection of the resulted sets to be prevented, thus, we will state the following theorem.

Table 1: The two matrices $M_{\{9/2\}}$ and $M_{\{9/3\}}$ where each of them defines nine contracting maps (every two rows define a map), needed for the random IFS procedure, resulting in the $\{9/2\}$ and $\{9/3\}$ fractal attractors shown in figure 3(a) and 3(b).

$M_{\{9/2\}}$			$M_{\{9/3\}}$		
0.2831	0	0.8660254	0.2578	0	0.8660254
0	0.2831	-0.5	0	0.2578	-0.5
0.2831	0	0.9848078	0.2578	0	0.9848078
0	0.2831	0.1736482	0	0.2578	0.1736482
0.2831	0	0.6427876	0.2578	0	0.6427876
0	0.2831	0.7660444	0	0.2578	0.7660444
0.2831	0	0	0.2578	0	0
0	0.2831	1	0	0.2578	1
0.2831	0	-0.642788	0.2578	0	-0.642788
0	0.2831	0.7660444	0	0.2578	0.7660444
0.2831	0	-0.984808	0.2578	0	-0.984808
0	0.2831	0.1736482	0	0.2578	0.1736482
0.2831	0	-0.866025	0.2578	0	-0.866025
0	0.2831	-0.5	0	0.2578	-0.5
0.2831	0	-0.34202	0.2578	0	-0.34202
0	0.2831	-0.939693	0	0.2578	-0.939693
0.2831	0	0.3420201	0.2578	0	0.3420201
0	0.2831	-0.939693	0	0.2578	-0.939693

Theorem 2. *If we have a strictly self-similar fractal set obtained as an attractor of IFS, where n -attracting points lie on S^1 , so that they are the vertices of a $\{n/m\}$ star-polygon, and where the attraction towards these points is $P = P(n, m)$ given by equation (1), then this fractal set is not-self-intersecting if and only if $m \in [n/4, n/4 + 1]$, which uniquely defines P for a given n .*

Proof. For clarity, one must look at figure 4 where with red is denoted the scaled down polygon towards A_{m+1} , self-similar to the original one. Although, it has 9 vertices, it must be considered as n/m star-polygon, because we will only use geometrical properties that are independent of n and m . For this purpose we must find out the following angles: $\angle A'MA_{m+1}$ and $\angle O_bMA_{m+1}$.

We already found that $\angle LA_{m+1}M = (m-1)\pi/n$ and therefore
 $\angle MA_{m+1}O_b = \angle O_bA_{m+1}A_{2m+1} = \pi/2 - \pi/n - (m-1)\pi/n \Rightarrow$
 $\Rightarrow \angle LA_{m+1}A_{2m+1} = 2(\pi/2 - \pi/n - (m-1)\pi/n) + (m-1)\pi/n = \pi - 2\pi/n - (m-1)\pi/n \Rightarrow$
 $\Rightarrow \angle LA_{m+1}A_{2m+1} = \frac{\pi}{n}(n-m-1)$. On the other hand due to the symmetry of the scaled polygon (in red) $\angle LA_{m+1}A_{2m+1} = \angle A_{m+1}MA'$ since $\angle A_{m+1}MN = \angle MA_{m+1}A_{2m+1}$ and $\angle NMA' = \angle MA_{m+1}L$. $\angle O_bMA_{m+1} = \pi/2 + (m-1)\pi/n$ as an exterior angle for $\triangle MLA_{m+1}$.

Now, note that the scaled polygon towards the A_{m+1} vertex (in red) reflected across the O_bL line segment will result in the scaled polygon towards the A_m vertex (in blue); see also figure 2. This is true because the O_bL represents an axis of symmetry for the initial polygon and it contains point M which is a common point for both the scaled polygons towards the A_m and A_{m+1} vertices. Now we can deduce that these two scaled polygons will not intersect with each other if the vertices A' and A'' stay together with A_{m+1} on the same side with respect to the O_bL axis. Then, $\angle O_bMA_{m+1} \geq \angle A_{m+1}MA'$ and $\angle LMA_{m+1} \geq \angle A_{m+1}MA'' \Rightarrow$

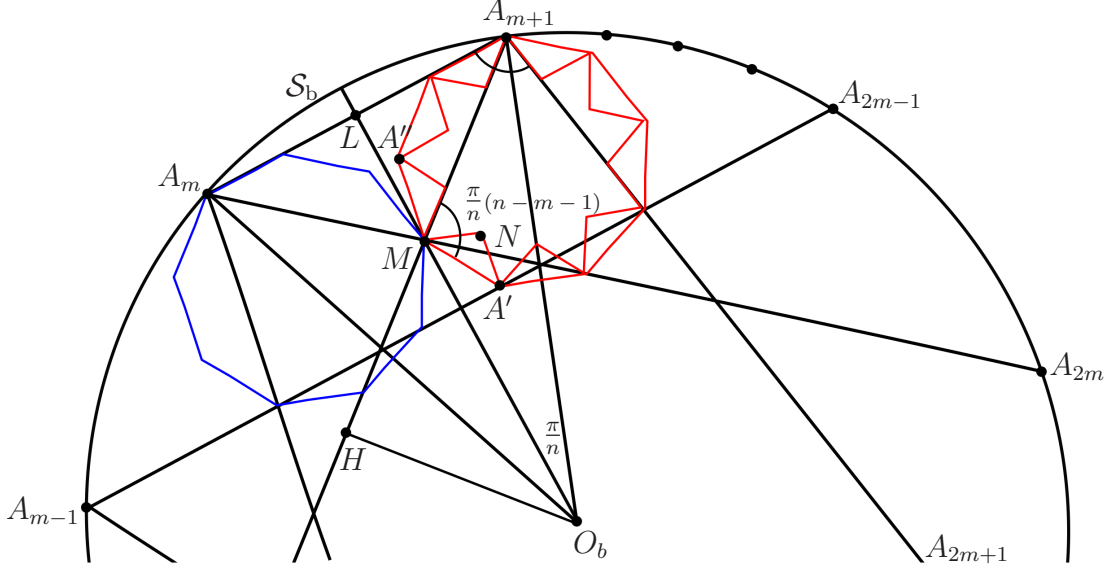


Figure 4: Sketch of $\{n/m\}$ star-polygon circumscribed in \mathcal{S}_b together with the scaled down polygon towards the A_{m+1} vertex (in red) and its mirror image across the line O_bL (in blue) which is equivalent to the scaled down polygon towards the A_m vertex.

$$\begin{aligned}
\angle O_bMA_{m+1} &\geq \angle A_{m+1}MA' & \angle LMA_{m+1} &\geq \angle A_{m+1}MA'' & (2) \\
\pi/2 + (m-1)\pi/n &\geq \pi - 2\pi/n - (m-1)\pi/n & \pi/2 - (m-1)\pi/n &\geq (m-1)\pi/n \\
(4m-4)/2n &\geq (n-4)/2n & 1/2 &\geq 2(m-1)/n \\
m &\geq n/4 & n/4 + 1 &\geq m
\end{aligned}$$

Thus, if the resulted fractal does not self-intersect, then $n/4 \geq m \geq n/4 + 1$, which uniquely defines m except when n can be divided by 4 without residual. At the same time, if the strict inequalities of equations (2) hold, this ensures that both of the vertices A' and A'' stay on the right hand side of O_bL line segment (see figure 4) \Rightarrow their mirror images with respect to O_bL will stay on the left hand side of O_bL . Otherwise, if A' and A'' were to cross the O_bL segment becoming on its left hand side, the two polygons would intersect with each other and this intersection would be repeated everywhere since the resulted fractal is strictly self-similar. Finally, if A' or A'' lies on O_bL and the two scaled polygon have a common side MA' or MA'' , then one of the equations (2) must be with a sign for equality.

$$\begin{aligned}
P &= \frac{\sin(\frac{\pi}{n})}{2 \cos(\frac{(m-1)\pi}{n}) \sin(\frac{m\pi}{n})} \\
P &= P_1(n, m) \text{ for } n = 4v \text{ and } m = v & P &= P_2(n, m) \text{ for } n = 4v \text{ and } m = v + 1 \\
P_1 &= \frac{\sin(\frac{\pi}{4v})}{2 \cos(\frac{(v-1)\pi}{4v}) \sin(\frac{v\pi}{4v})} & P_2 &= \frac{\sin(\frac{\pi}{4v})}{2 \cos(\frac{v\pi}{4v}) \sin(\frac{(v+1)\pi}{4v})} \\
P_1 &= \frac{\sin(\frac{\pi}{4v})}{2 \cos(\frac{(v-1)\pi}{4v}) \sin(\frac{\pi}{4})} & P_2 &= \frac{\sin(\frac{\pi}{4v})}{2 \cos(\frac{\pi}{4}) \sin(\frac{(v+1)\pi}{4v})} \\
P_1 &= \frac{\sin(\frac{\pi}{4v})}{\sqrt{2} \cos(\frac{(v-1)\pi}{4v})} & P_2 &= \frac{\sin(\frac{\pi}{4v})}{\sqrt{2} \sin(\frac{(v+1)\pi}{4v})} \\
P_1 &= \frac{\sin(\frac{\pi}{4v})}{\sqrt{2} \cos(\frac{v\pi}{4v}) \cos(\frac{\pi}{4v}) + \sqrt{2} \sin(\frac{v\pi}{4v}) \sin(\frac{\pi}{4v})} & P_2 &= \frac{\sin(\frac{\pi}{4v})}{\sqrt{2} \sin(\frac{v\pi}{4v}) \cos(\frac{\pi}{4v}) + \sqrt{2} \cos(\frac{v\pi}{4v}) \sin(\frac{\pi}{4v})} \\
P_1 &= \frac{\sin(\frac{\pi}{4v})}{\cos(\frac{\pi}{4v}) + \sin(\frac{\pi}{4v})} & P_2 &= \frac{\sin(\frac{\pi}{4v})}{\cos(\frac{\pi}{4v}) + \sin(\frac{\pi}{4v})} & (3)
\end{aligned}$$

Therefore, n must be divided by 4 without residual because $m \in \mathbb{N}$. Thus, when n is divided by 4 without residual and the scaling ratio is $P = P(n, m)$ from equations (2), then each of the scaled polygons has two common vertices with both of the adjacent scaled polygons.

The case when n is divided by 4 without residual and $m \in [n/4, n/4+1]$ implies that equation (1) produces two values for P . We will compute those values $P(4v, v)$ and $P(4v, v + 1)$, where $n = 4v$ for some $v > 0, v \in \mathbb{N}$; see equations (3). Equations (3) clearly show that $P(n, n/4) = P(n, n/4+1)$, when 4 divides n without residual, which ensures the unique definition of $P(n, m)$ when the resulted fractals are non-self-intersecting. \square

Corollary 1. *The attractors of the IFS with n attracting points that are the vertices of $\{n, n/4\}$ and $\{n, n/4+1\}$ star-polygons and whose scaling ratios are $P(n, n/4)$ and $P(n, n/4+1)$, respectively, are identical and composed of star-polygons that have two vertices in common with each of the adjacent polygons.*

Remark 1. *Note that theorem 2 is stated for the specific type of self-similar fractal sets obtained using IFS where the attracting points are the vertices of a $\{n/m\}$ star-polygon and P is defined by n and m as given in equation (1). Thus, it does not exclude other kinds of non-self-intersecting star-polygonal fractal sets constructed in a different fashion.*

3.2 Fractal dimensions

Theorem 2 allow us to define $F_{\{n/m\}}$ as the IFS attractor produced from an initial equilateral $\{n/m\}$ -polygon with n contracting maps that scale towards the n -vertices of the initial $\{n/m\}$ -polygon with ratio $P(n, m)$. We ensured that the obtained self-similar fractal set $F_{\{n/m\}}$ is non-self-intersecting, which allows us to compute its Hausdorff dimension $dim_H F_{\{n/m\}}$ [2] by solving the following equation:

$$\sum_{i=1}^N c_i^{dim_H F_{\{n/m\}}} = 1 \quad (4)$$

where N indicates the amount of similarity maps S_i (see Theorem 1) and $0 < c_i < 1$ are the scaling ratios for each similarity.

Since $P(2, 1) = 1/2$, $dim_H F_{\{2/1\}} = -\ln(2)/\ln(P(2, 1)) = 1$ which means that the attractor of $F_{\{2/1\}}$ is the initial line segment that connects both vertices or one can think about the Cantor set with scale ratio $1/2$.

For the $F_{\{9/3\}}$ in figure 3(b) we have $9P(9, 3)^{dim_H F_{\{9/3\}}} = 1$ which lead to $dim_H F_{\{9/3\}} = -\ln(9)/\ln(P(9, 3)) \approx 1.6207585335597825$.

In the following figures 5, 6, 7 and 8 are shown the attractors of $F_{\{n/m\}}$ where $n = 3, 4, 5, 6, 7, 8, 10, 11, 12, 13, 14, 15, 16, 24$ and $m \in [n/4, n/4 + 1]$. The dimensions of the presented fractals are computed in the examples that follows every figure. One can recognize well known fractals in the cases of $n = 3, 4, 5, 6$ but the other examples are not that famous due to the need of a special ratio in order to be constructed.

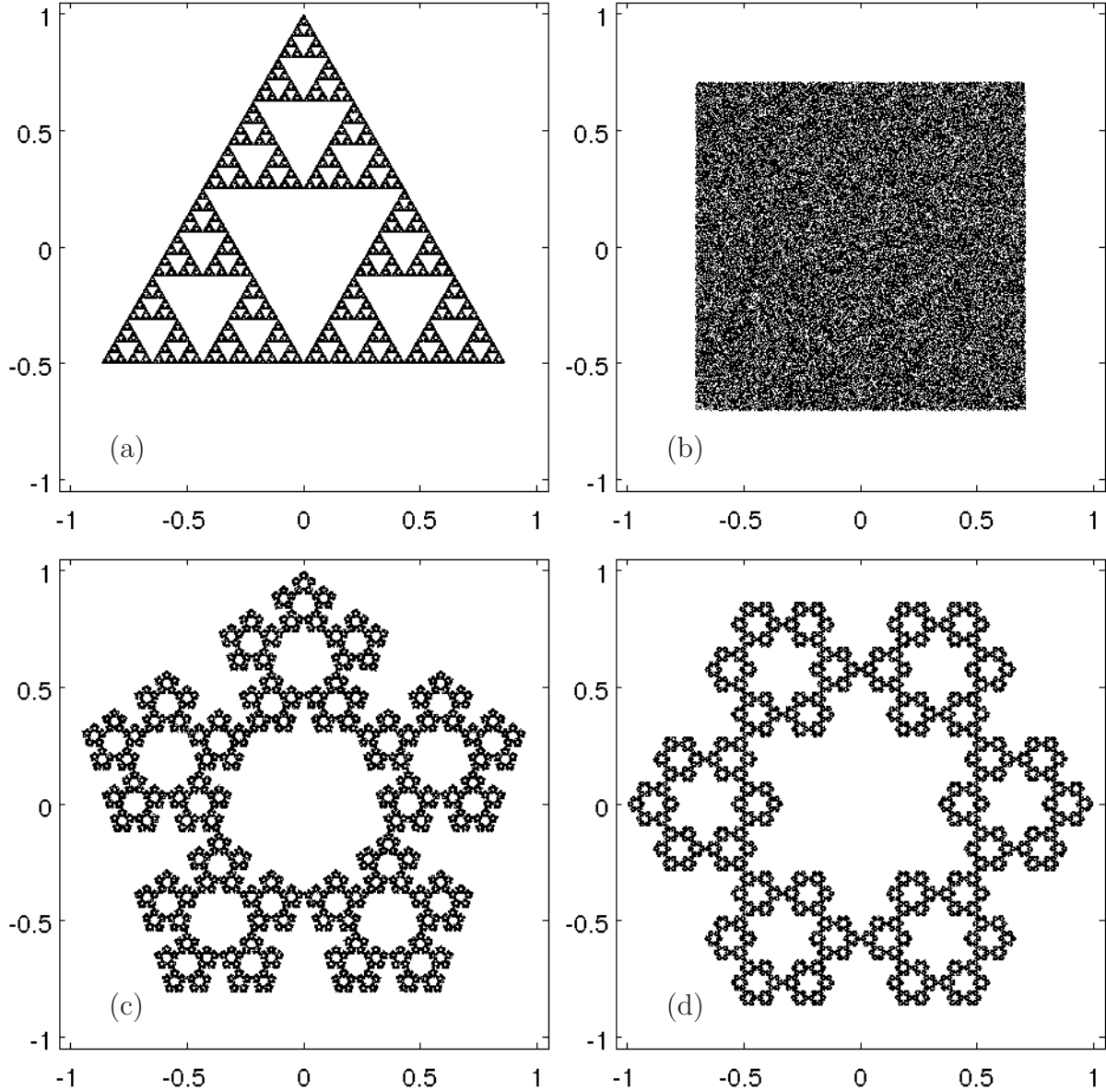


Figure 5: IFS generated fractal sets made of points that lie in $F_{\{3/1\}}$, $F_{\{4/2\}}$, $F_{\{5/2\}}$ and $F_{\{6/2\}}$ in subpanels (a), (b), (c) and (d), respectively.

Example 1. We will compute the Hausdorff dimensions of the attractors shown in figure 5:

- Figure 5(a) $\dim_H F_{\{3/1\}} = -\ln(3)/\ln(P(3, 1)) \approx 1.5849625007211563$
- Figure 5(b) $\dim_H F_{\{4/2\}} = -\ln(4)/\ln(P(4, 2)) = 2$
- Figure 5(c) $\dim_H F_{\{5/2\}} = -\ln(5)/\ln(P(5, 2)) \approx 1.6722759381845547$
- Figure 5(d) $\dim_H F_{\{6/2\}} = -\ln(6)/\ln(P(6, 2)) \approx 1.6309297535714573$

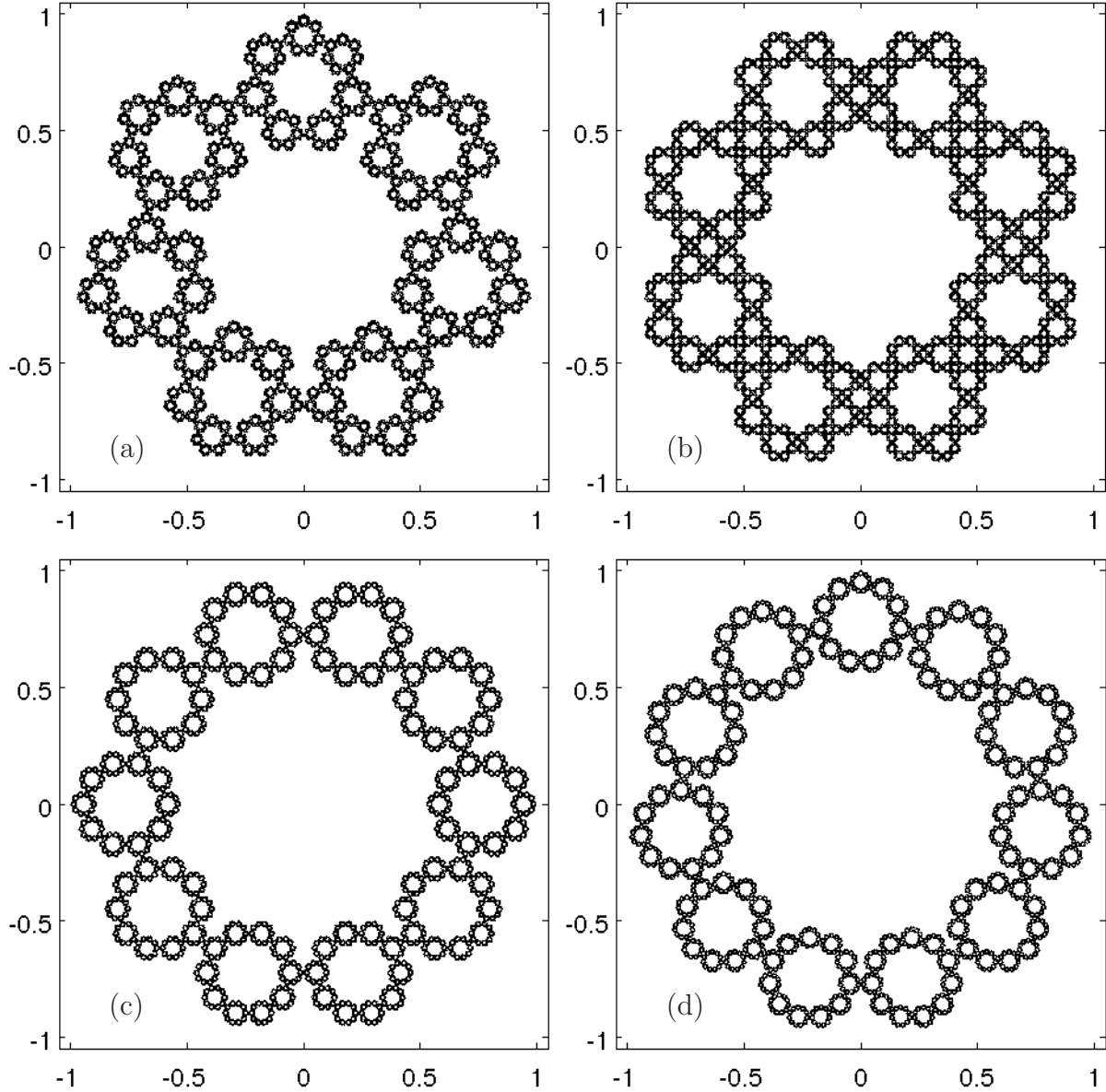


Figure 6: IFS generated fractal sets made of points that lie in $F_{\{7/2\}}$, $F_{\{8/3\}}$, $F_{\{10/3\}}$ and $F_{\{11/3\}}$ in subpanels (a), (b), (c) and (d), respectively. The IFS attractor of $F_{\{9/3\}}$ is shown in figure 3(b).

Example 2. We will compute the Hausdorff dimensions of the attractors shown in figure 6:

- Figure 6(a) $\dim_H F_{\{7/2\}} = -\ln(7)/\ln(P(7, 2)) \approx 1.6522616056918107$
- Figure 6(b) $\dim_H F_{\{8/3\}} = -\ln(8)/\ln(P(8, 3)) \approx 1.6934291475411138$
- Figure 6(c) $\dim_H F_{\{10/3\}} = -\ln(10)/\ln(P(10, 3)) \approx 1.5949906555938886$
- Figure 6(d) $\dim_H F_{\{11/3\}} = -\ln(11)/\ln(P(11, 3)) \approx 1.5911325154416658$

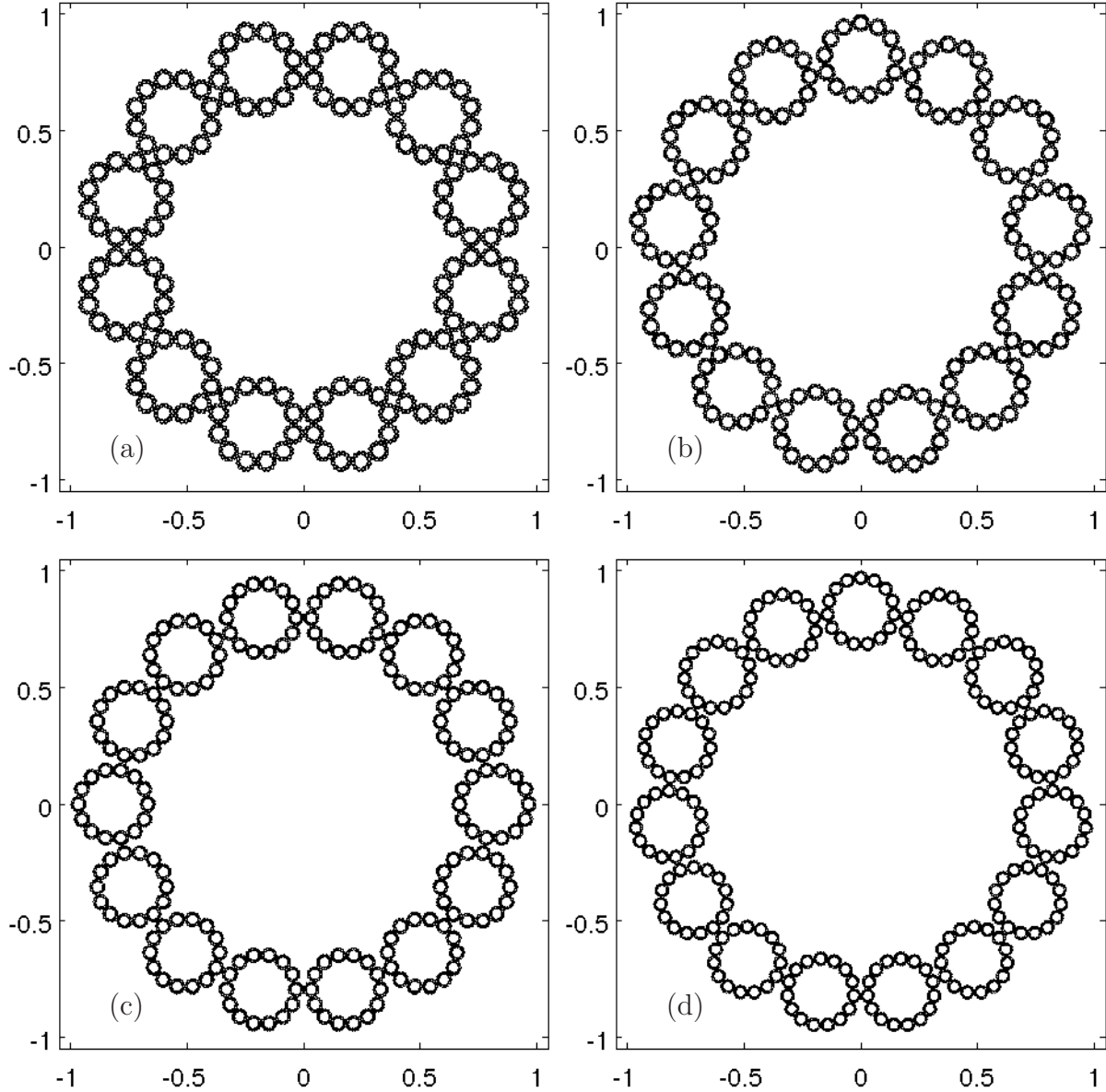


Figure 7: IFS generated fractal sets made of points that lie in $F_{\{12/4\}}$, $F_{\{13/4\}}$, $F_{\{14/4\}}$ and $F_{\{15/4\}}$ in subpanels (a), (b), (c) and (d), respectively.

Example 3. We will compute the Hausdorff dimensions of the attractors shown in figure 7:

- Figure 7(a) $\dim_H F_{\{12/4\}} = -\ln(12)/\ln(P(12, 4)) \approx 1.598670034685813$
- Figure 7(b) $\dim_H F_{\{13/4\}} = -\ln(13)/\ln(P(13, 4)) \approx 1.5653005271788485$
- Figure 7(c) $\dim_H F_{\{14/4\}} = -\ln(14)/\ln(P(14, 4)) \approx 1.5490615012592472$
- Figure 7(d) $\dim_H F_{\{15/4\}} = -\ln(15)/\ln(P(15, 4)) \approx 1.5430579163288531$

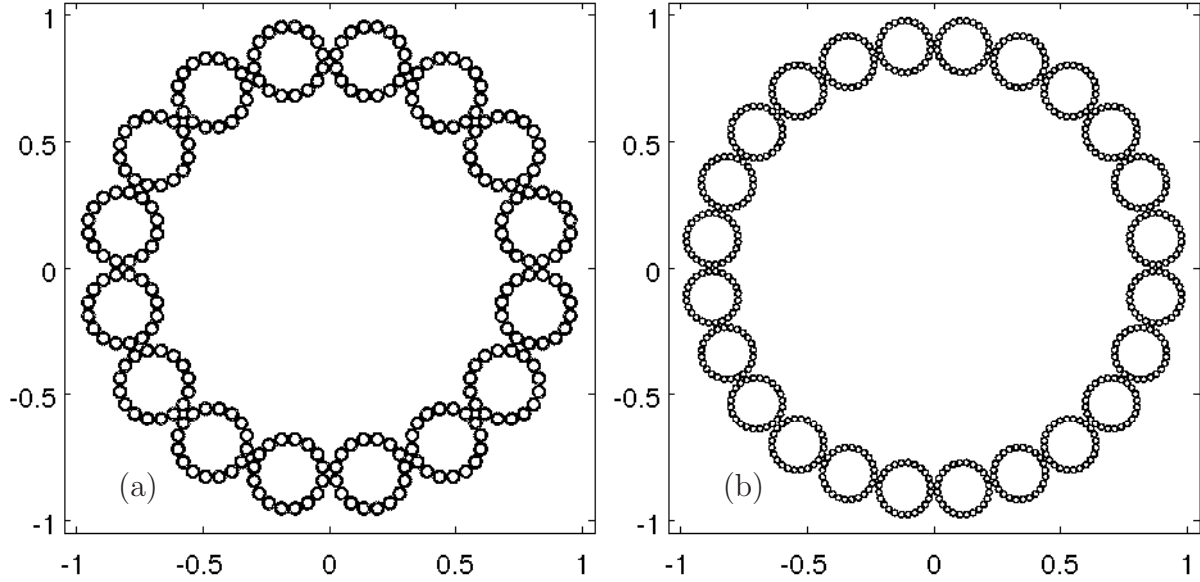


Figure 8: IFS generated fractal sets made of points that lie in $F_{\{16/5\}}$ and $F_{\{24/7\}}$ in subpanels (a) and (b), respectively.

Example 4. We will compute the Hausdorff dimensions of the attractors shown in figure 8:

- Figure 8(a) $\dim_H F_{\{16/5\}} = -\ln(16)/\ln(P(16, 5)) \approx 1.5434949184823248$
- Figure 8(b) $\dim_H F_{\{24/7\}} = -\ln(24)/\ln(P(24, 7)) \approx 1.4772930562556852$

Also, the $\dim_H F_{\{n/m\}}$ for $n \in [17, 50]$ and $m \in [n/4, n/4 + 1]$ are as follows:

$\{\dim_H F_{\{17/5\}}, \dim_H F_{\{18/5\}}, \dots, \dim_H F_{\{50/13\}}\} \approx \{1.5238, 1.5126, 1.5071, 1.5056, 1.4924, 1.4841, 1.4794, 1.4773, 1.4677, 1.4613, 1.4573, 1.4551, 1.4478, 1.4426, 1.4391, 1.437, 1.4312, 1.4269, 1.4239, 1.422, 1.4172, 1.4136, 1.4109, 1.4091, 1.4051, 1.402, 1.3997, 1.398, 1.3946, 1.3919, 1.3898, 1.3883, 1.3853, 1.3829\}$ Finally, for $n = 1e + 308$, $\dim_H F_{\{1e+308/2.5e+307\}} \approx 1.001622$.

Theorem 3. As n goes to infinity, $\dim_H F_{\{n/m\}}$ approaches 1

Proof. Let $s = \dim_H F_{\{n/m\}}$ then from $\lim_{n \rightarrow \infty} P = \lim_{n \rightarrow \infty} \frac{\sin(\pi/n)}{2\cos((m-1)\pi/n)\sin(m\pi/n)} =$
 $= \lim_{n \rightarrow \infty} \frac{\sin(\pi/n)}{2\cos(\pi/4)\sin(\pi/4)} = \lim_{n \rightarrow \infty} \sin(\pi/n) = \lim_{n \rightarrow \infty} \pi/n$ and $nP^s = 1$ we can deduce s .

Thus, $\lim_{n \rightarrow \infty} s = \lim_{n \rightarrow \infty} \frac{\ln(n)}{\ln(n/\pi)} = \infty/\infty$, hence $\lim_{n \rightarrow \infty} s = \lim_{n \rightarrow \infty} \frac{\frac{\partial \ln(n)}{\partial n}}{\frac{\partial \ln(n/\pi)}{\partial n}} = 1$ \square

As $F_{\{n/m\}}$ is inscribed in the same circle in which the initial $\{n/m\}$ -polygon is inscribed, a corollary of Theorem 3 is that as $n \rightarrow \infty$ the $F_{\{n/m\}}$ is going to be arbitrary close to the circle in which the initial $\{n/m\}$ -polygon is inscribed.

3.3 Exact drawing of the IFS iterations

All the figures above were drawn by using a random walk generator that draws points which lie in the IFS attractor [6, 2]. Another way of showing the attractor is by plotting large enough iteration (3th or 4th is usually enough) of the IFS where multiple scaled-down copies of the

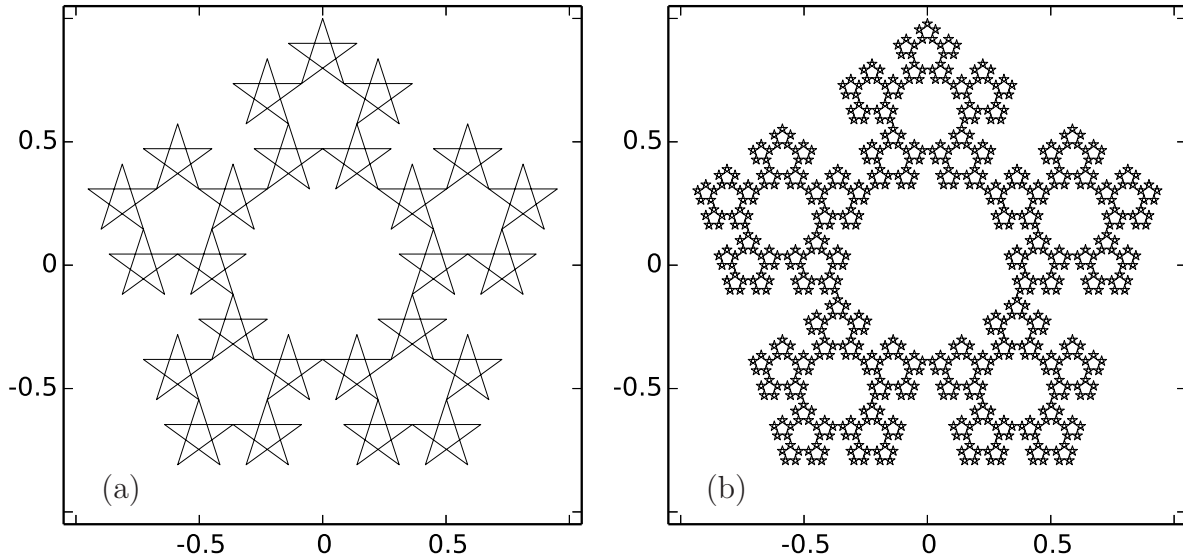


Figure 9: IFS with initial $\{5/2\}$ star-polygon where the second and the fourth iterations are shown in panels (a) and (b), respectively.

initial polygon are imaged. In figure 9 an example of this plotting approach is shown where in panel (b) the fourth iteration of the $\{5/2\}$ -polygon looks like figure 5(c) where the same attractor is produced by the random walk technique. In the next section we will use the latter technique more often for the sake of the clarity of the concepts presented.

4 The centre of the circle as an additional point of attraction

If we add the centre of the circle as another attracting point that the random generator takes into account, then we can produce non-self-intersecting fractal sets that cover a great amount of the area that is bounded by the unit circle. This result is due to the fact that the centre point adds to the IFS attractor (the invariant set) one more scaled copy of the initial star-polygon, hence we need an additional contracting map which we will call S_c . Moreover, if the scaling factor of the central point is carefully computed, one can exploit a number of different features of the star-polygons. Here we will give a few introductory examples.

Let us consider an initial polygon $\{3/1\}$, then $P(3,1) = 1/2$ and let us have a central map S_c with the same ratio $1/2$ and rotation $\pi/3$ added to the set of maps $\{S_1, S_2, S_3\}$. This will result in a triangular shape attractor with a Hausdorff dimension $dim_H F_{\{3/1\}}[L^1, \pi/3] = -\ln(4)/\ln(P(3,1)) = \ln(4)/\ln(2) = 2$. Thus, the only difference from the attractor shown in figure 5(b) will be the triangular shape.

We will present the IFS of the $\{5/2\}$ (see figure 10, Example 5) with an attracting centre, where the similarity map corresponding to the centre point has the same scaling factor $P(5,2)$ as the maps that correspond to the vertices of the initial $\{5/2\}$ -polygon. In figure 11 another IFS is shown and its dimension is computed in Example 6. This fractal has centre-map that not only scales, but also rotates the initial polygon at angle $\pi/5$ while keeping the ratio $P(5,2)$. Let us also see the IFS of the $\{6/2\}$ with an attracting centre, where the similarity map corresponding

to the centre point has a scaling factor $P(6, 2)$ and does not imply rotation, presented in figure 12 and Example 7.

From the dimensions computed in section 3.2 we can deduce that as n grows the scaling ratio $P(n, m)$, where $m \in [n/4, n/4 + 1]$ monotonically decreases and the resulting fractals shrink in dimension. Thus, if we want to increase n , but keep the attractors with a reasonably high dimension, we can no longer use the same ratio for the centre scaling map as in the cases for $n = 5$ and $n = 6$. Therefore, we will define different rules for the scaling ratio of the centre map S_c for any n , depending if it is odd or even and if S_c includes any rotation such as π/n or it does not.

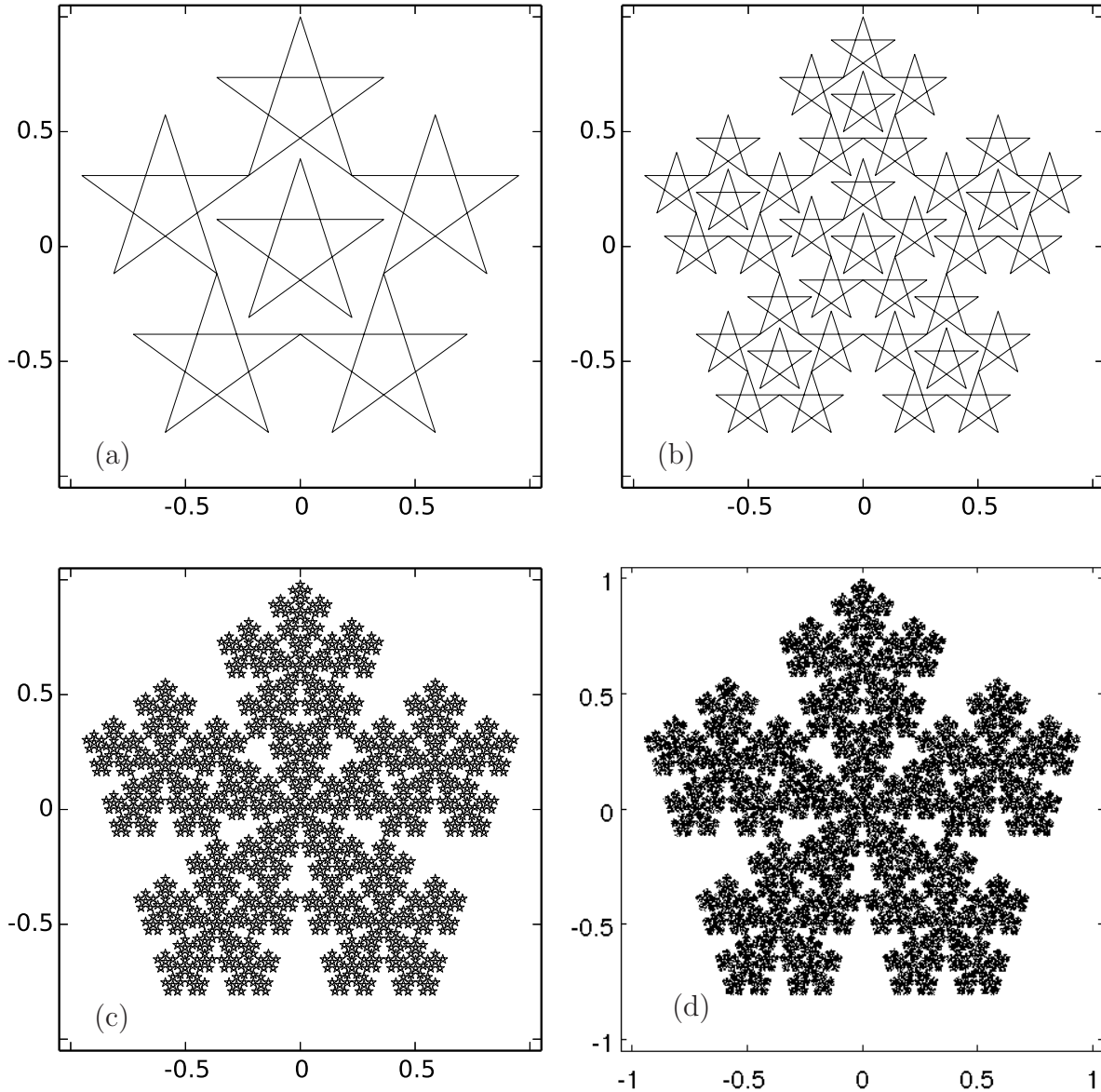


Figure 10: IFS with initial $\{5/2\}$ star-polygon where the central map S_c has no rotation and uses the ratio $P(5, 2)$. The first, the second and the fourth iterations are shown in panels (a), (b) and (c) respectively. 100000 points that lie on the attractor of the IFS are shown in panel (d).

Example 5. We will compute the Hausdorff dimensions of the attractor shown in figure 10(d):
 $\dim_H F_{\{5/2\}}[L^1, 0] = -\ln(6)/\ln(P(5, 2)) \approx 1.8617$

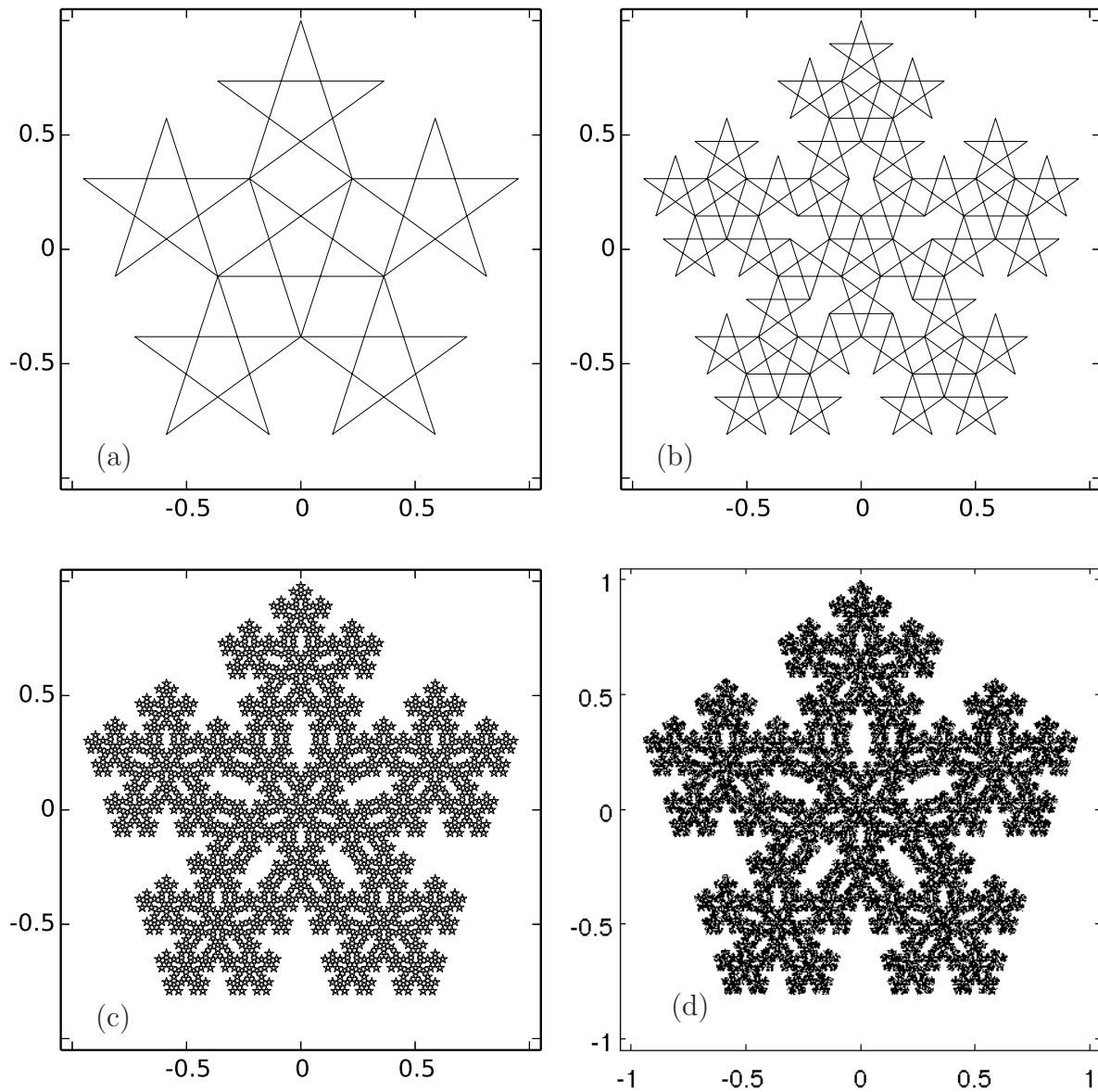


Figure 11: IFS with initial $\{5/2\}$ star-polygon where the central map S_c has rotation $\pi/5$ and uses the ratio $P(5, 2)$. The first, the second and the fourth iterations are shown in panels (a), (b) and (c) respectively. 100000 points that lie on the attractor of the IFS are shown in panel (d).

Example 6. We will compute the Hausdorff dimensions of the attractor shown in figure 11(d):
 $\dim_H F_{\{5/2\}}[L^1, \pi/5] = \dim_H F_{\{5/2\}}[L^1, 0] = -\ln(6)/\ln(P(5, 2)) \approx 1.8617$

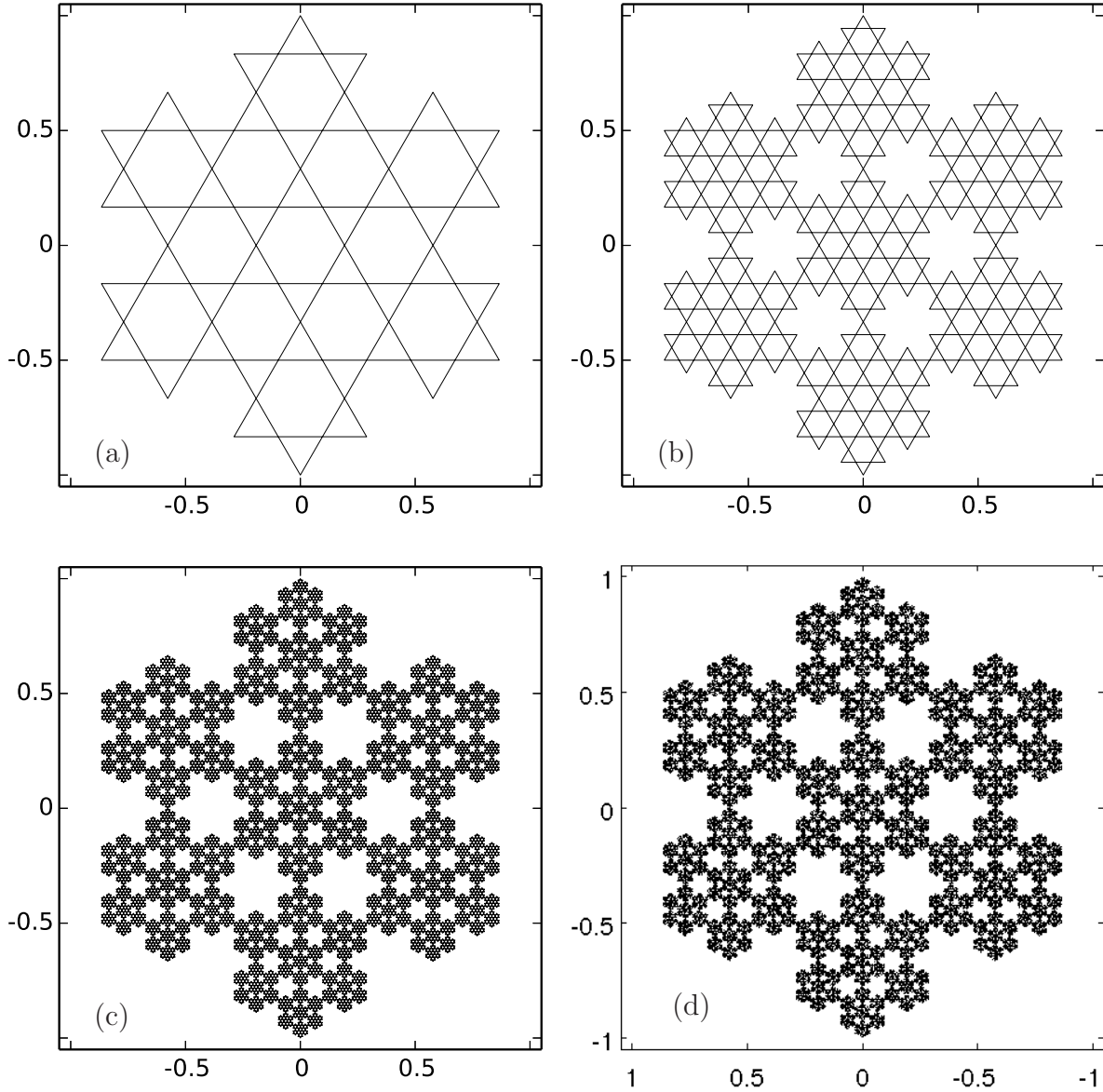


Figure 12: IFS with initial $\{6/2\}$ star-polygon where the central map S_c has no rotation and uses the ratio $P(6, 2)$. The first, the second and the fourth iterations are shown in panels (a), (b) and (c) respectively. 100000 points that lie on the attractor of the IFS are shown in panel (d).

Example 7. We will compute the Hausdorff dimensions of the attractor shown in figure 12(d):
 $\dim_H F_{\{6/2\}}[L^0, 0] = -\ln(7)/\ln(P(6, 2)) \approx 1.7712$

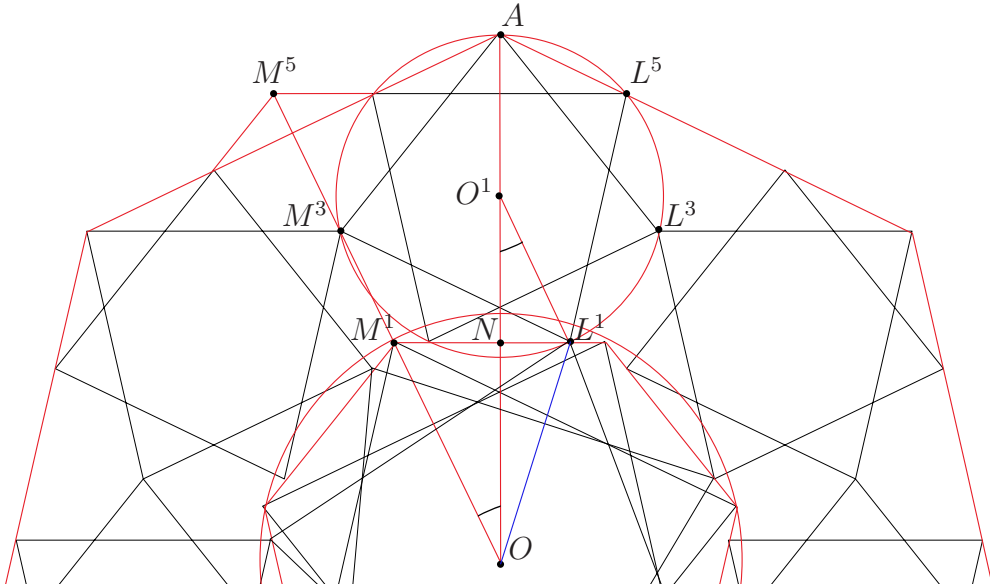


Figure 13: Sketch of a $\{7/2\}$ polygon IFS with a centre map after the first iteration. Shown is the way of computing of the ratio for the centre map.

In order to clearly show how the ratios of S_c are deduced, in figure 13 is sketched part of the IFS of $\{7/2\}$ -polygon when it is iterated only once. There are two centre polygons, one is rotated at angle $\pi/7$ (the one with a vertex at M^1) and another rotated at an angle to be computed later (with vertex L^1). Thus, the contraction map that scales the original $\{7/2\}$ -polygon towards the point O and images it in one of these two polygons includes rotation as well. Using the sketch in figure 13 we will show that some of the points M^i and L^i will be used as vertices of a central polygon that corresponds to a central map S_c , which can be used for non-self-intersecting polygonal IFS.

Let us construct the points $M^1, M^3, M^5, \dots, M^{2i+1}$ lying on the line that crosses the line-segment O^1O at angle $\pi/7$. This line is intersected by the line segments that start from the vertices L^1, L^3 and L^5 and are perpendicular to the line-segment O^1O resulting in the points M^1, M^3 and M^5 . Now we will define six different ratios P_c for the centre map S_c : OM^1/OA , OM^3/OA , OM^5/OA and OL^1/OA , OL^3/OA , OL^5/OA . All of them are defined by the angles $\angle OO^1L^l = l\pi/n$ where in general $l = 2i + 1$ for $i \geq 0, i \in \mathbb{Z}$ when the polygons are odd-sided and $l = 2i$ when the polygons are even-sided. For $l = 1, 3, 5$, $ON = OA - O^1A - O^1L^l \cos(l\pi/7)$ and $OM^l = ON / \cos(\pi/7)$, thus $OM^l/OA = 1 / \cos(\pi/7) - (O^1A/OA)(1 / \cos(\pi/7) - \cos(l\pi/7) / \cos(\pi/7))$. This equation also holds for $l = 7$, where $A \equiv L^7$ and if apply equation (1), so that $O^1A/OA = P(7, 2)$, then $OM^l/OA = 1 / \cos(\pi/7) - P(7, 2) / \cos(\pi/7) - P(7, 2) \cos(l\pi/7) / \cos(\pi/7)$. Also, if generalised for an arbitrary initial $\{n/m\}$ -polygon, it leads to the following equation:

$$\frac{OM^l}{OA} = \frac{1 - P(n, m) - P(n, m) \cos(l\pi/n)}{\cos(\pi/n)} \quad (5)$$

$$\angle O^1OM^l = \pi/n$$

$$0 \leq l \leq n, l = 2i \text{ if } n\text{-even}, l = 2i + 1 \text{ if } n\text{-odd}, i \geq 0, i \in \mathbb{Z}$$

Another ratio that may be used for the map S_c is OL^1/OA . Here $NL^1 = O^1L^1 \sin(\pi/7)$,

hence, $\tan(\angle O^1 O L^1) = \frac{O^1 L^1 \sin(\pi/7)}{OA - O^1 A - O^1 L^1 \cos(\pi/7)}$ which for an arbitrary l will become

$$\tan(\angle O^1 O L^l) = \frac{O^1 L^l \sin(l\pi/7)}{OA - O^1 A - O^1 L^l \cos(l\pi/7)}.$$

Now let us take into account that $O^1 L^l = O^1 A$ and $O^1 A/OA = P(7, 2)$, hence $\tan(\angle O^1 O L^l) = \frac{P(7, 2) \sin(l\pi/7)}{1 - P(7, 2) - P(7, 2) \cos(l\pi/7)}$. Finally, for an arbitrary initial $\{n/m\}$ -polygon we can deduce the angle $\angle O^1 O L^l$ and from $(OL^l)^2 = (NL^l)^2 + (ON)^2$ we can also deduce the ratio OL^l/OA as follows:

$$\frac{OL^l}{OA} = \sqrt{2P(n, m)(P(n, m) - 1)(1 + \cos(l\pi/n)) + 1} \quad (6)$$

$$\gamma(n, m, l) = \angle O^1 O L^l = \arctan \left(\frac{P(n, m) \sin(l\pi/n)}{1 - P(n, m) - P(n, m) \cos(l\pi/n)} \right)$$

$$0 \leq l \leq n, l = 2i \text{ if } n\text{-even}, l = 2i + 1 \text{ if } n\text{-odd}, i \geq 0, i \in \mathbb{Z}$$

Now we can look back at figures 10, 11 and 12 and understand how they are constructed. In example 5, figure 10, the contraction ratio of S_c is OL^1/OA , and the attractor of the IFS is denoted as $F_{\{5/2\}}[L^1, 0]$, where 0 indicates the angle of rotation that S_c has. In this case of $\{5/2\}$ -polygon $OM^1/OA = OL^1/OA$, so it does not matter if L^1 or M^1 is used for the notation. In the other examples where $OL^l/OA = OM^l/OA$, again L^l will be used as notation. In example 6, figure 11 the contraction ratio of S_c is again OL^1/OA , but here we have rotation at angle $\pi/5$, thus the attractor of the IFS is denoted as $F_{\{5/2\}}[L^1, \pi/5]$. And finally in example 7, figure 12 the contraction ratio of S_c is OL^0/OA and the attractor of the IFS is denoted $F_{\{6/2\}}[L^0, 0]$.

4.1 Even n

In this subsection we will take a close look at the IFS that originates from even sided star-polygons. Firstly, we should note that the same way as $F_{\{6/2\}}[L^0, 0]$, for any even n , $F_{\{2i/m\}}[L^0, 0]$ will always be a non-self-intersecting attractor if $m \in [n/4, n/4 + 1]$ and $i \in \mathbb{N}$. Now, the first example has $\{6/2\}$ as initial polygon, and S_c has scaling ratio OL^2/OA and rotation $\pi/6$. The resulting fractal can be seen in figure 14, where from the random generated attractor, see panel (d), we can expect the exact dimension of 2. Indeed, this is analytically proven in the computations of example 8. Similarly, the constructions and the attractors of $F_{\{8/2\}}[L^2, \frac{\pi}{8}]$ and $F_{\{8/3\}}[L^2, \frac{\pi}{8}]$ are shown in figures 15 and 16. They have equal dimension computed in example 9. Another pair of attractors that have central map and originate from $\{8/2\}$ -star polygon are the $F_{\{8/2\}}[L^0, 0]$ and $F_{\{8/3\}}[L^0, 0]$ shown in figures 17 and 18. They have equal dimension computed in example 10. The last four examples of attractors clearly show that the scaling ratio and the number of the vertices are the parameters that define the attractor of the IFS.

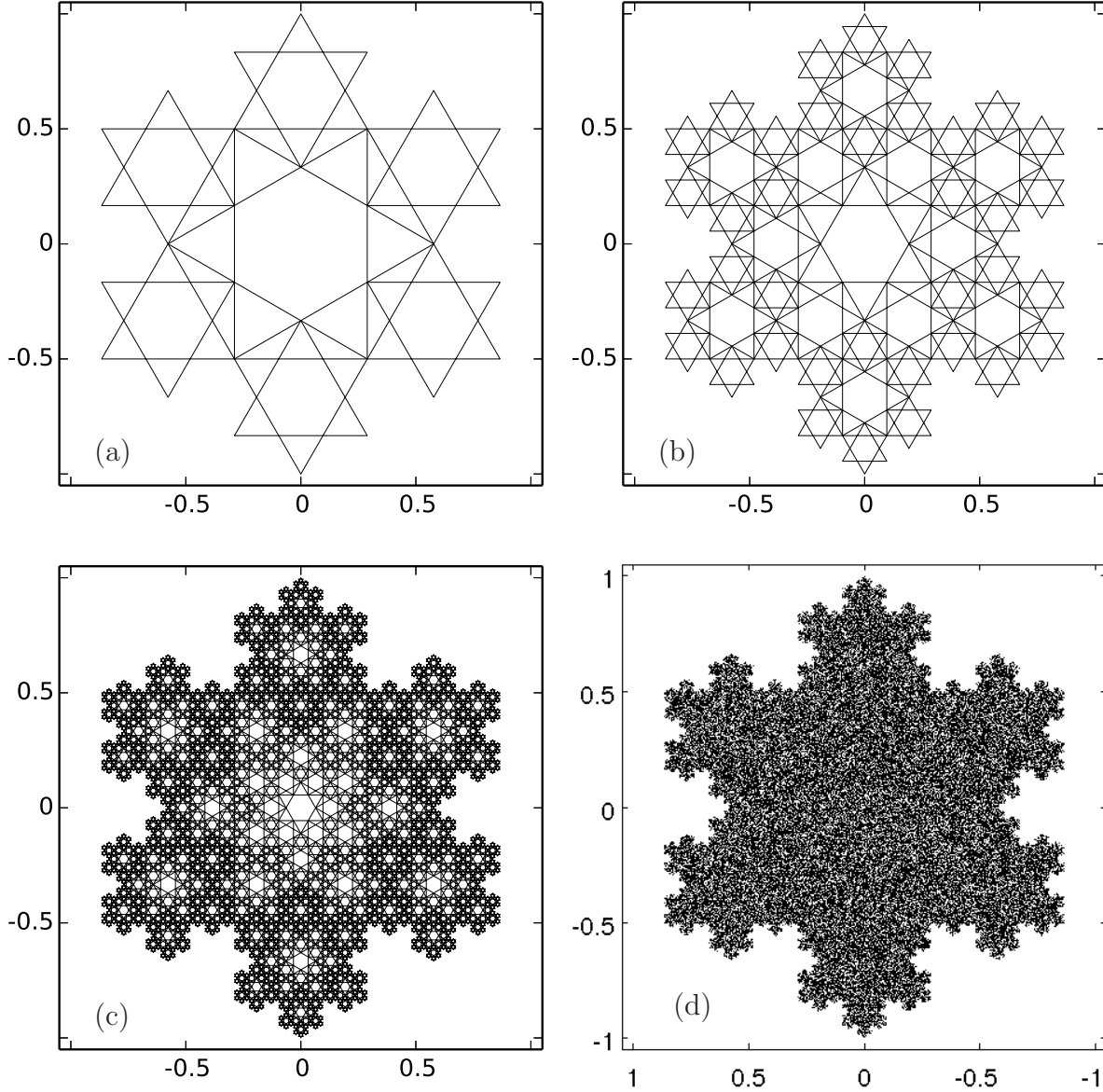


Figure 14: IFS with initial $\{6/2\}$ star-polygon where S_c has scaling ratio OL^2/OA and rotation $\pi/6$. The first, the second and the fourth iterations are shown in panels (a), (b) and (c) respectively. 100000 points that lie on the attractor of the IFS are shown in panel (d).

Example 8. We will compute the Hausdorff dimensions of the attractor shown in figure 14(d):

$$6P(6, 2)^{\dim_H F_{\{6/2\}}[L^2, \frac{\pi}{6}]} + \sqrt{2P(6, 2)(P(6, 2) - 1)(1 + \cos(2\pi/6)) + 1}^{\dim_H F_{\{6/2\}}[L^2, \frac{\pi}{6}]} = 1$$

$$6(1/3)^{\dim_H F_{\{6/2\}}[L^2, \frac{\pi}{6}]} + \sqrt{(1/3)^{\dim_H F_{\{6/2\}}[L^2, \frac{\pi}{6}]}} = 1. \text{ Let } y = \sqrt{(1/3)^{\dim_H F_{\{6/2\}}[L^2, \frac{\pi}{6}]}}$$

Hence, $6y^2 + y - 1 = 0$ and $y_{1,2} = 1/3; -1/2$, therefore as $y \geq 0$

$$\sqrt{(1/3)^{\dim_H F_{\{6/2\}}[L^2, \frac{\pi}{6}]}} = 1/3 \rightarrow \dim_H F_{\{6/2\}}[L^2, \frac{\pi}{6}] = 2.$$

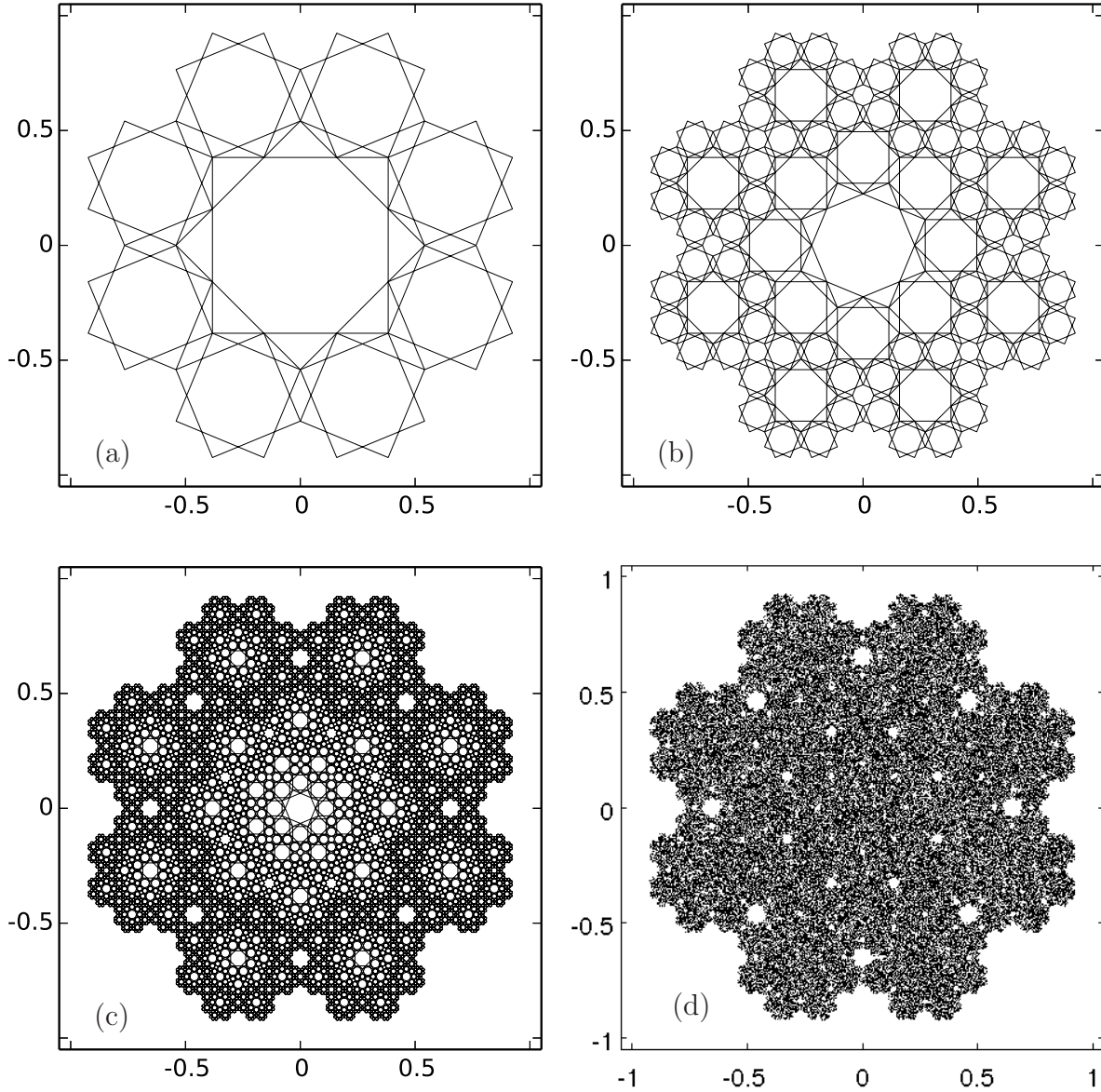


Figure 15: IFS with initial $\{8/2\}$ star-polygon where S_c has scaling ratio OL^2/OA and rotation $\pi/8$. The first, the second and the fourth iterations are shown in panels (a), (b) and (c) respectively. 100000 points that lie on the attractor of the IFS are shown in panel (d).

Example 9. *The Hausdorff dimensions of the attractor shown in figure 15(d) is $\dim_H F_{\{8/2\}}[L^2, \frac{\pi}{8}] \approx 1.9799$*

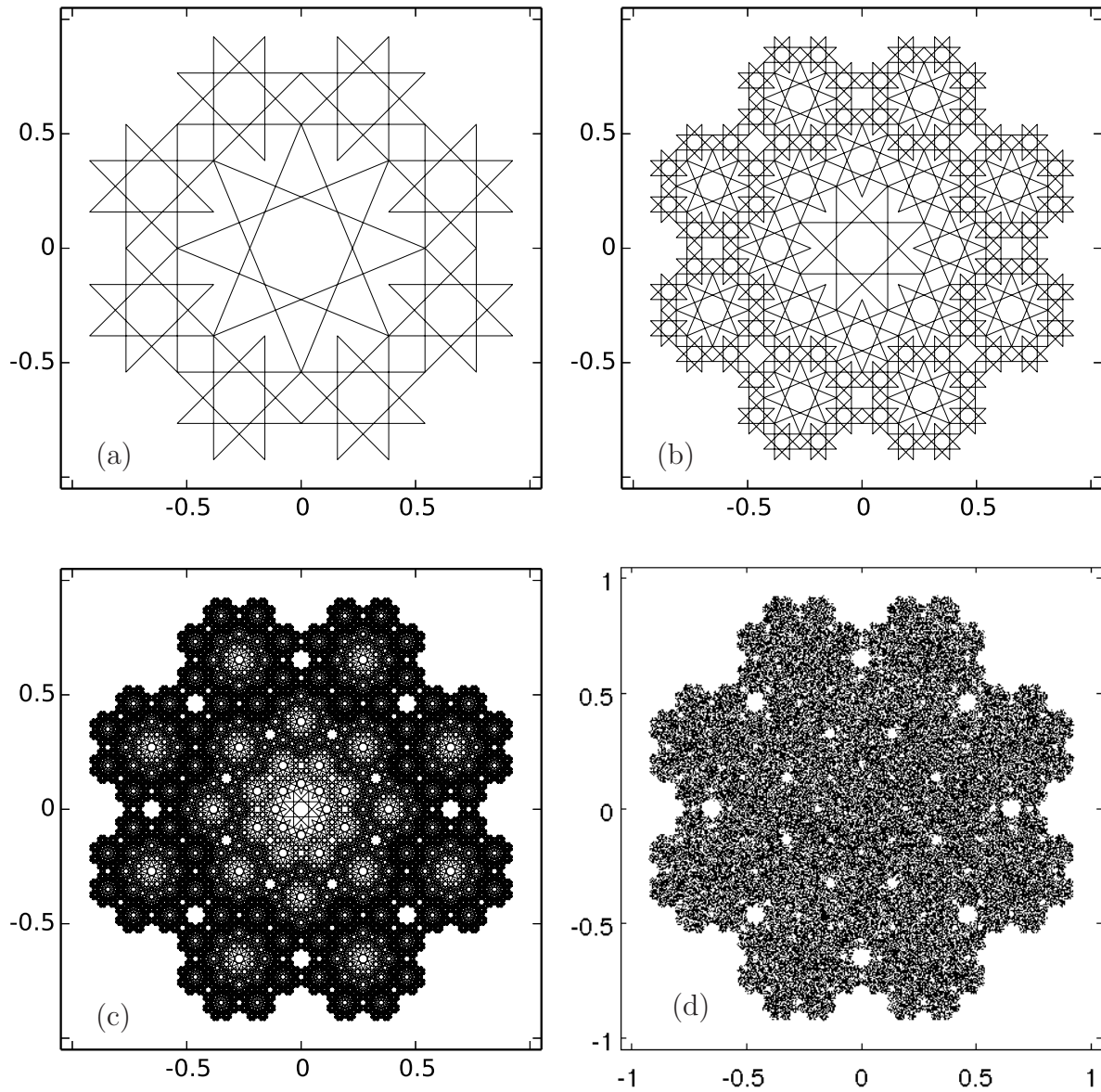


Figure 16: IFS with initial $\{8/3\}$ star-polygon where S_c has scaling ratio OL^2/OA and rotation $\pi/8$. The first, the second and the fourth iterations are shown in panels (a), (b) and (c) respectively. 100000 points that lie on the attractor of the IFS are shown in panel (d).

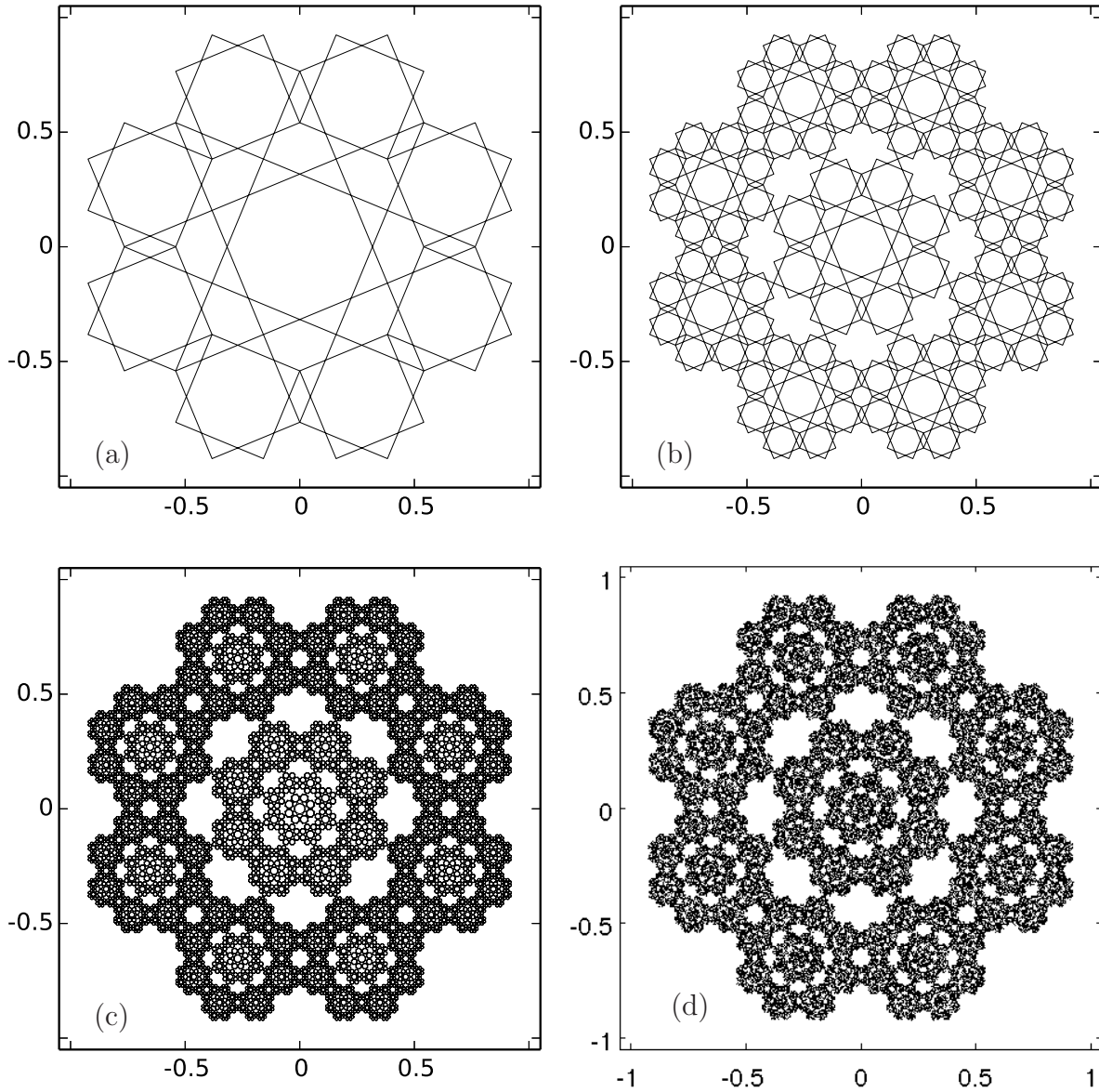


Figure 17: IFS with initial $\{8/2\}$ star-polygon where S_c has scaling ratio OL^0/OA and no rotation. The first, the second and the fourth iterations are shown in panels (a), (b) and (c) respectively. 100000 points that lie on the attractor of the IFS are shown in panel (d).

Example 10. *The Hausdorff dimensions of the attractor shown in figure 17(d) is $\dim_H F_{\{8/2\}}[L^0, 0] \approx 1.8678$*

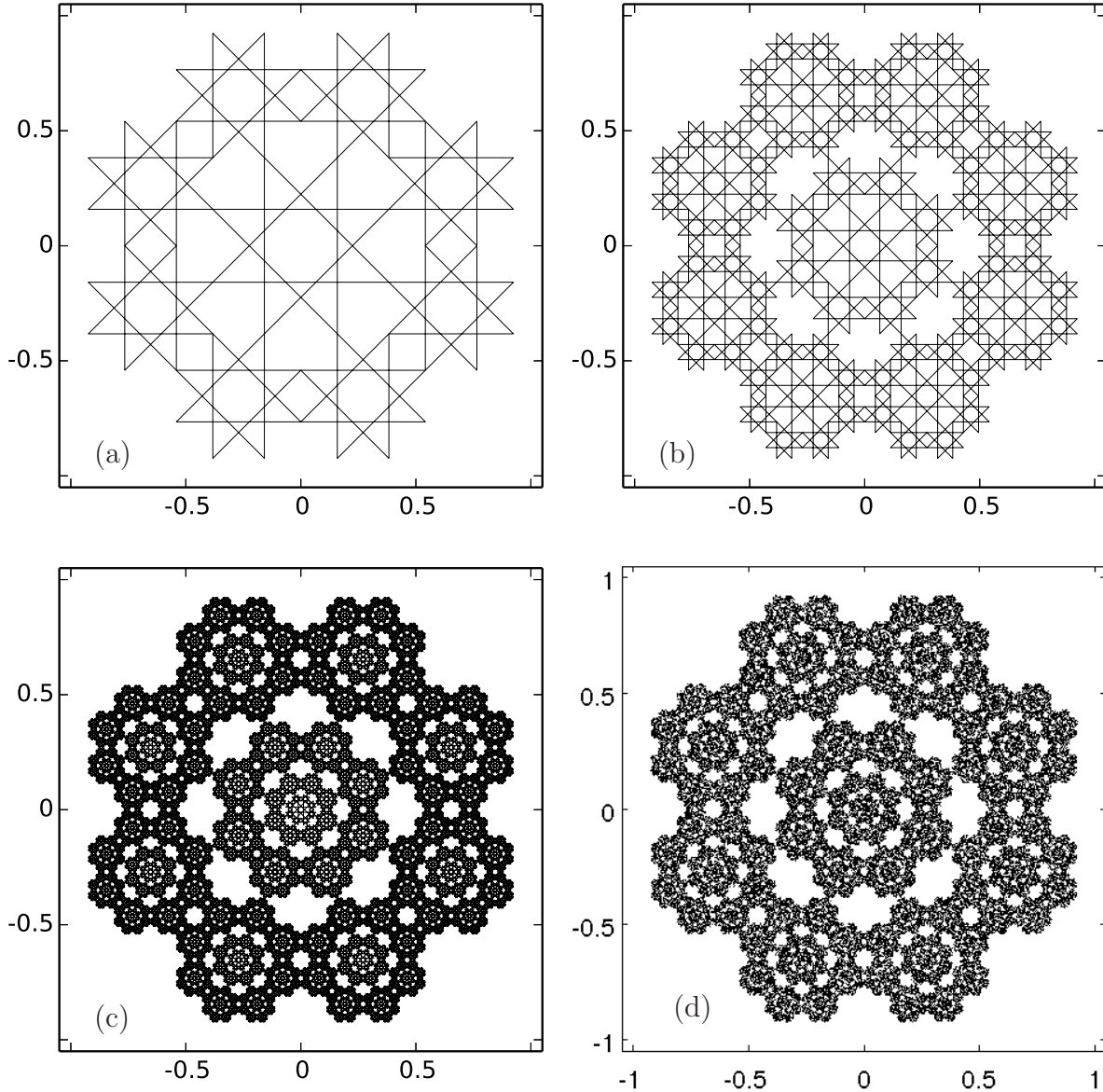


Figure 18: IFS with initial $\{8/3\}$ star-polygon where S_c has scaling ratio OL^0/OA and no rotation. The first, the second and the fourth iterations are shown in panels (a), (b) and (c) respectively. 100000 points that lie on the attractor of the IFS are shown in panel (d).

4.2 Odd n

In this subsection we will take a close look at the IFS that originates from odd-sided star-polygons. The first example has $\{7/2\}$ as an initial polygon and S_c has a scaling ratio OM^1/OA and rotation $\pi/7$; see Eqs. (5). The resulting fractal can be seen in figure 19, where the first, the second and the fourth iterations are in panels (a), (b) and (c), while the randomly generated attractor is in panel (d). The Hausdorff dimension of the attractor $F_{\{7/2\}}[M^1, \pi/7]$ is computed in example 11 to be 1.8773. Another fractal that originates from a $\{7/2\}$ -polygon is shown in figure 20. Here the scaling ratio is OL^1/OA and the angle of rotation is computed using equations (6), which leads to polygons that meet at their vertices. The dimension of

$F_{\{7/2\}}[L^1, \gamma(7, 2, 1)]$ is computed in example 12 to be 1.8564.

The technique that uses the ratio OL^1/OA and the angle from equations (6) can also be used for producing non-intersecting self-similar fractals for any odd n . Therefore, for any n we can generate a n -flake which will be either $F_{\{n/m\}}[L^0, 0]$ if n is even or $F_{\{n/m\}}[L^1, \gamma(n, m, 1)]$ if n is odd.

4.3 The dimension of ∞ -flake

For any $n, m \in [n/4, n/4 + 1]$ and $i \in \mathbb{N}$, by construction if $n = 2i$ then $F_{\{n/m\}}[L^0, 0]$ is non-self-intersecting, and by construction if $n = 2i + 1$ then $F_{\{n/m\}}[L^1, \gamma(n, m, 1)]$ is non-self-intersecting. Therefore, equations (1), (4) and (6) can be used for the corresponding $\dim_H F_{\{n/m\}}[L^0, 0]$ and $\dim_H F_{\{n/m\}}[L^1, \gamma(n, m, 1)]$ to be obtained.

Theorem 4. *As n goes to infinity, $\dim_H F_{\{n/m\}}[L^0, 0]$ and $\dim_H F_{\{n/m\}}[L^1, \gamma(n, m, 1)]$ approach 2.*

Proof. Both dimensions can be deduced from the equation

$$nP(n, m)^s + \sqrt{2P(n, m)(P(n, m) - 1)(1 + \cos(l\pi/n)) + 1}^s = 1,$$

where s denotes $\dim_H F_{\{n/m\}}[L^0, 0]$ or $\dim_H F_{\{n/m\}}[L^1, \gamma(n, m, 1)]$. The latter equation can be modified to

$$P^s = \frac{1}{n} - \frac{\sqrt{2P(n, m)(P(n, m) - 1)(1 + \cos(l\pi/n)) + 1}^s}{n},$$

from where:

$$\begin{aligned} s &= \lim_{n \rightarrow \infty} \frac{\ln \left(\frac{1}{n} - \frac{\sqrt{2P(n, m)(P(n, m) - 1)(1 + \cos(l\pi/n)) + 1}^s}{n} \right)}{\ln(P)} = \\ &= \lim_{n \rightarrow \infty} \frac{\ln \left(\frac{1}{n} - \frac{\sqrt{4P(n, m)(P(n, m) - 1) + 1}^s}{n} \right)}{\ln(P)} = \\ &= \lim_{n \rightarrow \infty} \frac{\ln \left(\frac{1}{n} - \frac{(1 - 2P)^s}{n} \right)}{\ln(P)} = \lim_{n \rightarrow \infty} \frac{\ln \left(\frac{1}{n} - \frac{(1 - 2\pi/n)^s}{n} \right)}{\ln(\pi/n)} \end{aligned}$$

Let us substitute $\nu = \pi/n$, hence

$$\begin{aligned} s &= \lim_{\nu \rightarrow 0} \frac{\ln \left(\frac{\nu}{\pi} (1 - (1 - 2\nu)^s) \right)}{\ln(\nu)} = \lim_{\nu \rightarrow 0} \frac{\ln \left(\frac{\nu}{\pi} \right)}{\ln(\nu)} + \lim_{\nu \rightarrow 0} \frac{\ln(1 - (1 - 2\nu)^s)}{\ln(\nu)} = \\ &= 1 + \frac{-\infty}{-\infty} = 1 + \lim_{\nu \rightarrow 0} \frac{2s\nu(1 - 2\nu)^{s-1}}{1 - (1 - 2\nu)^s} = 1 + \lim_{\nu \rightarrow 0} \frac{2s\nu(1 - (s-1)2\nu + O(2))}{1 - (1 - s2\nu + O(2))} = \\ &= 1 + \lim_{\nu \rightarrow 0} \frac{2s\nu + O(2)}{2s\nu + O(2)} = 2 \end{aligned}$$

□

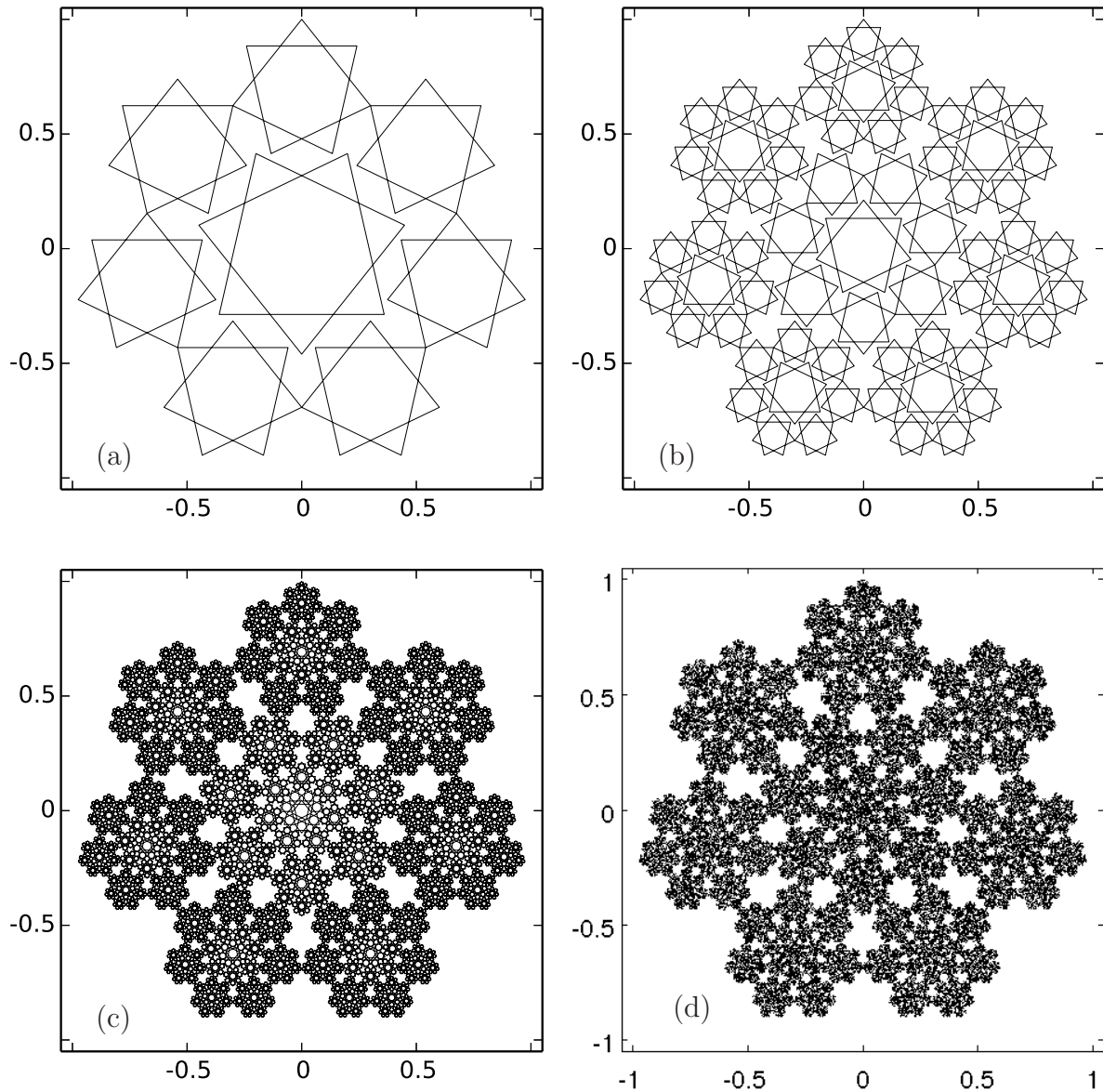


Figure 19: IFS with initial $\{7/2\}$ star-polygon where S_c has scaling ratio OM^1/OA and rotation $\pi/7$. The first, the second and the fourth iterations are shown in panels (a), (b) and (c) respectively. 100000 points that lie on the attractor of the IFS are shown in panel (d).

Example 11. The Hausdorff dimensions of the attractor shown in figure 19(d) is $\dim_H F_{\{7/2\}}[M^1, \frac{\pi}{7}] \approx 1.8773$

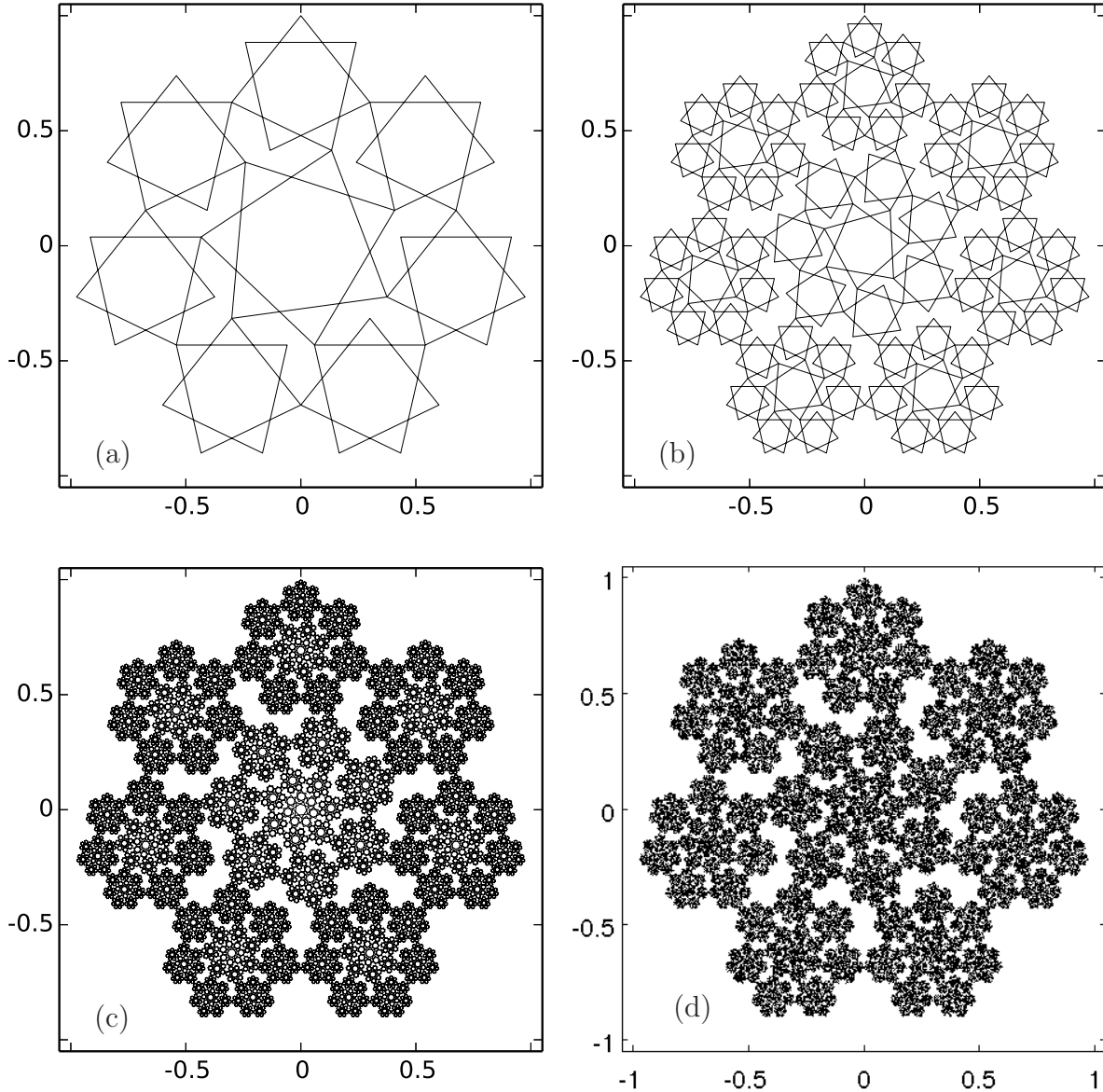


Figure 20: IFS with initial $\{7/2\}$ star-polygon where S_c has scaling ratio OL^1/OA and rotation $\gamma(7, 2, 1)$ radians. The first, the second and the fourth iterations are shown in panels (a), (b) and (c) respectively. 100000 points that lie on the attractor of the IFS are shown in panel (d).

Example 12. *The Hausdorff dimensions of the attractor shown in figure 20(d) is $\dim_H F_{\{7/2\}[L^1, \gamma(7, 2, 1)]} \approx 1.8564$*

5 Special cases and equivalent IFS attractors

As in the previous sections, here we assume $n \geq 2$, $n \in \mathbb{Z}$, $m \in \mathbb{Z}$, $0 \leq m < n$, and $i \in \mathbb{Z}$, $i \geq 0$. Let us now review the developed notation and how many of the well known fractals can be associated with it. Firstly, we can say that the Cantor set results as an IFS attractor if $n = 2$ and $P = 1/3$. As we saw in figure 5(a), the Sierpinski Triangle comes out when $n = 3$ and $P = P(3, 1) = 1/2$ or $F_{\{3/1\}}$ and the Sierpinski Hexagon when $n = 6$ and $P = P(6, 2) = 1/3$ or

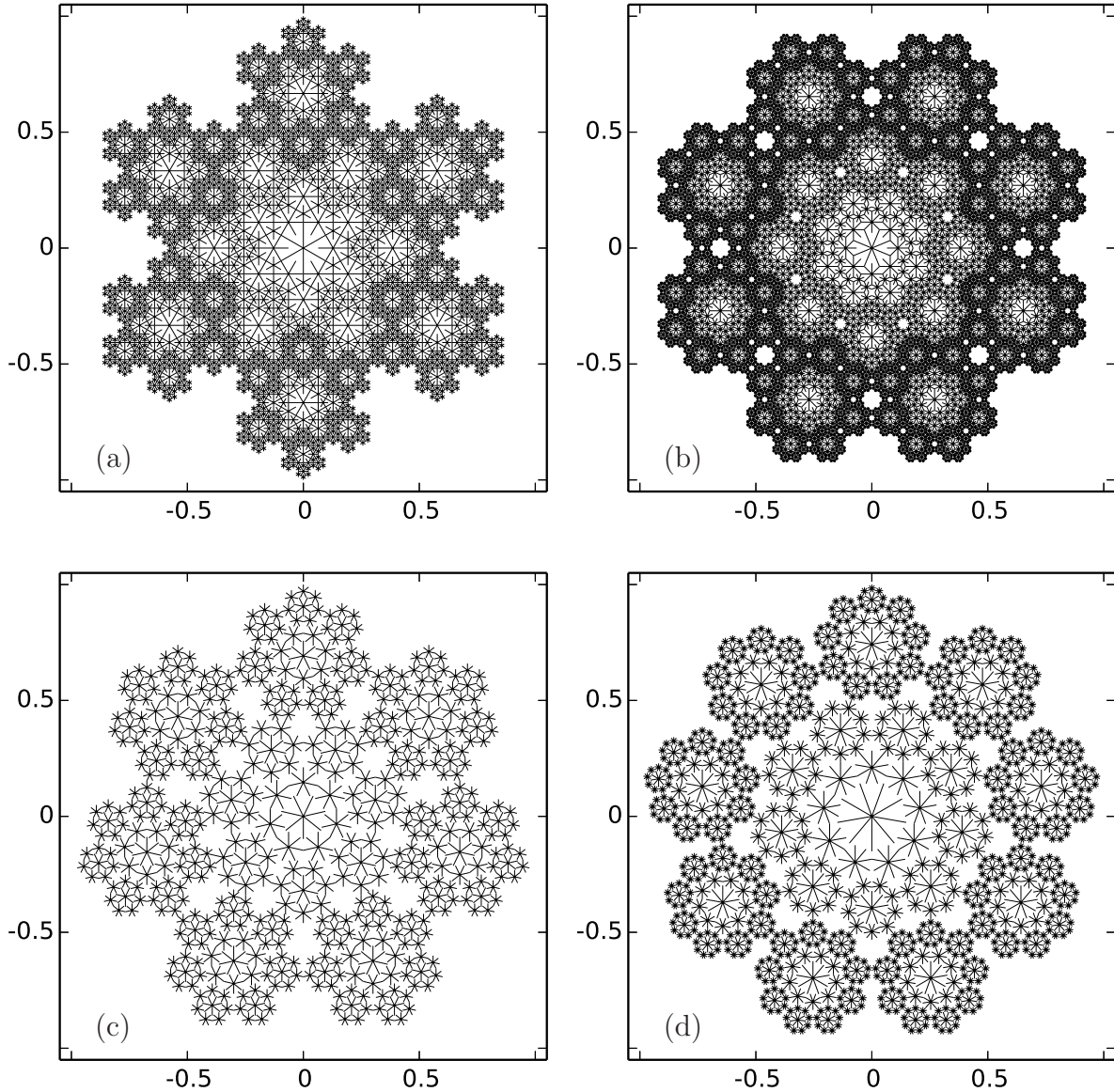


Figure 21: In subpanels (a) and (b) we can see the third iteration of the IFS that originate from $\{6/3\}$ and $\{8/4\}$, respectively. Both S_c have scaling ratio OL^2/OA , where in panel (a) the rotation is $\pi/6$ and in (b) it is $\pi/8$. In subpanels (c) and (d) we can see the third iteration of the IFS that originate from $\{7/3.5\}$ and $\{9/4.5\}$, respectively. Both S_c have scaling ratio OM^1/OA , where in panel (c) the rotation is $\pi/7$ and in (d) it is $\pi/9$.

$F_{\{6/2\}}$. The Greek Cross fractal appears when $n = 4$ and $P = P(4, 2) = 1/2$ or $F_{\{4/2\}}$, while for $n = 4$ and $P < 1/2$ the invariant set for a Horseshoe map is produced. The Sierpinski Pentagon appears for $n = 5$ and $P = P(5, 2) = 1/(1 + \text{golden ratio})$ or $F_{\{5/2\}}$. When the centre map S_c is taken into account, the Vicsec fractal can be produced when $n = 4$ and $P = P_c = 1/3$. Also, the Pentaflake and the Hexaflake are shown in figures 11 and 12 as $F_{\{5/2\}}[L^1, 0]$ and $F_{\{6/2\}}[L^0, 0]$, respectively.

However, the attractors of the special cases mentioned above do not originate from an unique star-polygons because if we generate random points on the attractor of the IFS, the image is defined by the maps $\{S_i\}$; see theorem 1. Therefore, if we do not alter P and n , the IFS-attractors with any initial $\{n, m\}$ -polygon will be the same. Thus, we can assume that every attractor that originates from a $\{2i, m\}$ -polygon is equivalent to the attractor of the IFS that originate from the $\{2i, i\}$ -polygon, where the ratios and the rotations of the maps $\{S_1, \dots, S_{2i}, S_c\}$ are kept the same as the ones used for the IFS of the $\{2i, m\}$ -polygon. However, when the exact polygons are plotted, as in section 4, due to the impossibility for infinite iterations to be realised, the integer m also plays its role. Two such examples are shown in figure 21, where in panels (a) and (b) the third iterations of the IFS of $F_{\{6/3\}}[L^2, \frac{\pi}{6}]$ and $F_{\{8/4\}}[L^2, \frac{\pi}{8}]$ are realised respectively. One can see the difference with figures 14, 15 and 16 where $F_{\{6/2\}}[L^2, \frac{\pi}{6}]$, $F_{\{8/2\}}[L^2, \frac{\pi}{8}]$ and $F_{\{8/3\}}[L^2, \frac{\pi}{8}]$ are shown.

In the case of odd $n = 2i + 1$ we do not have a star-polygon composed of n line-segments that cross each other at the centre and are inscribed in all the $\{2i+1, m\}$ -polygons in the same way as the $\{2i, i\}$ -polygon is inscribed in any $\{2i, m\}$ -polygon. Therefore, we will construct such polygons as the star of $2i + 1$ line segments that start from the centre of a $2i + 1$ regular polygon and end up at its vertices. Let us denote this figure as $\{2i + 1, i + 1/2\}$ -star polygon. As the $\{2i + 1, i + 1/2\}$ -polygon is inscribed in all the $\{2i + 1, m\}$ -polygons we can generalise that any attractor that originates from a $\{n, m\}$ -polygon is equivalent to the attractor of the IFS that originates from the $\{n, n/2\}$ -polygon where the ratios and the rotations of the maps $\{S_1, \dots, S_n, S_c\}$ are kept the same as the ones used for the IFS of the $\{n, m\}$ -polygon. Two such examples are shown in figure 21, where in panels (c) and (d) the third iterations of the IFS of $F_{\{7/3.5\}}[M^1, \frac{\pi}{7}]$ and $F_{\{9/4.5\}}[M^1, \frac{\pi}{9}]$ are realised. One can see the difference with figures 19 where $F_{\{7/3\}}[M^1, \frac{\pi}{7}]$ was shown.

Example 13. *If the fractal figure 21(d) is infinitely iterated the attractor will have Hausdorff dimension: $\dim_H F_{\{9/4.5\}}[M^1, \frac{\pi}{9}] \approx 1.8879$*

Unlike the cases of $n = 3, 5, 7$ and 9 , where the $F_{\{n/\frac{n}{2}\}}[M^1, \frac{\pi}{n}]$ is a non-self intersecting fractal with the copies of the initial $\{n/\frac{n}{2}\}$ -polygon osculating with each other, for $n = 2i + 1$ when $n \geq 11$, the scaled copies stop osculating and with the increase of the iterations they do not fill up the space in the most effective way. The same effect appears when we take $F_{\{n/\frac{n}{2}\}}[L^2, \frac{\pi}{n}]$ for $n = 2i$ when $n \geq 10$. Thus, the problem of finding scaling ratio for the S_c for every $n \geq 10$ where the rotation of S_c is equal to π/n stays as an open problem. This is an important question due to the fact that the fractals that originate from an n -gon with rotation of S_c equal to π/n could have dimensions very close or equal to 2 ; see examples 8 and 9.

Conclusion

The present paper develops a universal technique that allows any star-polygon to be used for the construction of non-self intersecting fractal (Sierpinski n -gon or n -flake) by using IFS through

random walk or through an exact scaling. Along the proposed scaling ratios, the Matlab code for IFS random walk fractal generation is provided so that someone interested in studying the geometry of this class of fractals could use it. Important dimensions are computed, namely the dimension of the Sierpinski ∞ -gon is proved to be 1, the dimension of the ∞ -flake to be 2, and the dimension of $F\{6, 2\}[L^2, \pi/6]$ to be 2 as well. It is also shown, that by using random walk IFS generator, identical attractors may result from different initial star-polygons. The proposed study can be extended if rotations are applied not only to the S_c map, but to the S_i maps as well. However, this is still an ongoing research in development.

The techniques for construction and the provided ratios needed for the dimensions of the presented class of fractals is important not only for mathematicians, but also for engineers and other scientists who may be interested in fractal-shaped devices or who study the fractal shapes of nature. With the advanced precision of the fabrication technology polyflakes may become an important design for devices such as antennas or chemical mixers for fuel cells, batteries, etc. Also, fractal shapes are applicable in any kind of wave absorbers where the wave could be a sound wave, electromagnetic signal, light, caused by turbulent flow, etc. In other words, fractal designs are going to be part of the future physical devices at all scales and, hence, the research focused on fractal-shaped figures is important for many innovation processes.

Acknowledgement

First of all I would like to thank my Geometry teacher Tanya Stoeva for the dedicated classes during the years at National Gymnasium of Natural Sciences and Mathematics "Lyubomir Chakalov" which still help me to overcome problems in the most intuitive way. Also, I would like to thank my family and friends for the support.

Appendix (Matlab random generator)

```
% name: Vassil Tzanov
% function 'frac' that takes the matrix C,
% C =  $\begin{bmatrix} A_1 & b_1 \\ A_2 & b_2 \\ \vdots & \vdots \\ A_n & b_n \end{bmatrix}$ 
% Ai are matrices 2x2 ,bi are vectors 2x1, which are the i-th linear function in the "IFS"
% k defines the amount of points that we want to be plotted
% on the attractor defined by C; the function 'frac' can plot fractals
% with central polygon rotated at angle rot; the central map must be defined by
% the last two rows of C; if there is no central map, rot has to be defined as 0
function Fractal = frac(C,k,rot)

% verification of C
D=size(C);
n=D(1)/2;
if D(2)~=3 | floor(n)~=n
    Fractal = 'Bad input size';
```

```

else

% computation of the determinants of the matrices A
for i=1:n
    dets(i)=abs(det(C((2*i-1):(2*i),1:2)));
end
dets=dets';

% if some determinant is zero we have to add a small value, because
% we do not like this function to be executed with zero probability
dets=max(dets, max(dets)/(25*n));

% the determinant are divided on their sum so we derive a probability vector
dets = dets/sum(dets);

% the vector prob is defined as
% prob = [0, dets(1), dets(1)+dets(2), . . . , dets(1)+...+dets(n-1)]
% then "sum(prob<rand)" gives a random integer between 1 and n
% that we use in order to randomly choose one of the n-th functions
de=dets(1);
prob(1)=0;
for i=2:n
    prob(i)=de;
    de=de+dets(i);
end

% computations of the points' coordinates and filling the matrix Fractal
x=[0;0];
Fractal=zeros(2,k+20);
for j=1:(k+20)
    int=sum(prob<rand);
    % one of the functions is randomly chosen
    i=int;
    % matrix computation of  $t * x + (1 - t) * y$ , where  $x$  is
    % the current point and  $y$  is the point towards which  $x$  is attracted
    % if  $i$  corresponds to the last row,
    % a rotation at  $rot$  radians around  $[0,0]$  must be executed
    if i==n
        x=[cos(rot),-sin(rot);sin(rot),cos(rot)]*x;
        x=C((2*i-1):(2*i),1:2)*x+(diag([1,1],0)-
-C((2*i-1):(2*i),1:2))*C((2*i-1):(2*i),3);
        Fractal(:,j)=x;
    else
        x=C((2*i-1):(2*i),1:2)*x+(diag([1,1],0)-
-C((2*i-1):(2*i),1:2))*C((2*i-1):(2*i),3);
        Fractal(:,j)=x;
    end
end

```

```

end

% the points of the matrix Fractal are plotted
Fractal=Fractal(:,21:(k+20));
plot(Fractal(1,:),Fractal(2,:),'k.','MarkerSize',1)
axis('equal')
end
end

```

References

- [1] B. Mandelbrot *The Fractal Geometry of Nature*, Freeman (1982)
- [2] K. Falconer, *Fractal Geometry - Mathematical foundations and applications*, Wiley (1990).
- [3] H. Coxeter, *Regular Polytopes*, Pitman (1947)
- [4] K. Dennis, S. Schlicker, *Sierpinski N-Gons*, Pi Mu Epsilon Journal, 10, 2 (1995)
- [5] M. Zuhair, S. Alam, *Generating fractals from regular n-gons*, Proceedings of National Conference on Nonlinear Systems and Dynamics, Kolkata, India, 2009
- [6] R. Devaney, *Chaos, Fractals, and Dynamics: Computer Experiments in Mathematics*, Addison-Wesley (1990).
- [7] H. Peitgen, H. Jurgens, D. Saupe, *Chaos and Fractals: New Frontiers of Science*, Springer-Verlag (2004)